Journal of Organometallic Chemistry 751 (2014) 399–411

Contents lists available at ScienceDirect

Journal of Organometallic Chemistry

journal homepage: www.elsevier.com/locate/jorganchem

A comparative study of the reactivity of the lightly stabilized cluster $[Os_3(CO)_8\{\mu_3\text{-}Ph_2PCH_2P(Ph)C_6H_4\}(\mu\text{-}H)]$ towards tri(2-thienyl)-, tri(2-furyl)- and triphenyl-phosphine

Arun K. Raha [a], Md. Nazim Uddin [a], Shishir Ghosh [a,b], Abdur R. Miah [a], Michael G. Richmond [c], Derek A. Tocher [b], Ebbe Nordlander [d], Graeme Hogarth [b,*], Shariff E. Kabir [a,*]

[a] Department of Chemistry, Jahangirnagar University, Savar, Dhaka 1342, Bangladesh
[b] Department of Chemistry, University College London, 20 Gordon Street, London WC1H OAJ, UK
[c] Department of Chemistry, University of North Texas, 1155 Union Circle, Box 305070, Denton, TX 76203, USA
[d] Inorganic Chemistry Research Group, Chemical Physics, Center for Chemistry and Chemical Engineering, Lund University, P.O. Box 124, SE-22100 Lund, Sweden

ARTICLE INFO

Article history:
Received 28 May 2013
Received in revised form
9 August 2013
Accepted 12 August 2013

Keywords:
Triosmium
Phosphines
Addition reactions
Isomerization
Carbon-phosphorus bond cleavage
DFT studies

ABSTRACT

Reactions of the lightly stabilized triosmium cluster $[Os_3(CO)_8\{\mu_3\text{-}Ph_2PCH_2P(Ph)C_6H_4\}(\mu\text{-}H)]$ with tri(2-thienyl)phosphine (PTh_3) and tri(2-furyl)phosphine (PFu_3) are described and compared to analogous reactions with PPh_3. At room temperature, a number of products are isolated: $[Os_3(CO)_{10}(\mu\text{-dppm})]$ from CO addition, $[Os_3(CO)_8(PR_3)\{\mu_3\text{-}Ph_2PCH_2P(Ph)C_6H_4\}(\mu\text{-}H)]$ from phosphine addition, $[Os_3(CO)_9(PR_3)(\mu\text{-dppm})]$ from phosphine and CO addition and $[Os_3(CO)_8(PR_3)_2(\mu\text{-dppm})]$ from addition of two equivalents of phosphine. The latter are shown by NMR and X-ray diffraction to exist as 1,2-isomers, whereby one phosphine is bound to the non-dppm-substituted center and the second shares an osmium atom with one end of the diphosphine. Heating 1,2-$[Os_3(CO)_8(PTh_3)_2(\mu\text{-dppm})]$ at 100 °C results in its clean isomerization to the 1,1-isomer in which both monodentate phosphines are located on the same osmium atom. Prolonged heating of $[Os_3(CO)_8(PR_3)_2(\mu\text{-dppm})]$ (R = Th, Ph) at 110 °C gives $[Os_3(CO)_9(PR_3)(\mu\text{-dppm})]$ and the new lightly stabilized clusters $[Os_3(CO)_7(PR_3)\{\mu_3\text{-}Ph_2PCH_2P(Ph)C_6H_4\}(\mu\text{-}H)]$, the latter being formed by loss of phosphine and CO with concurrent metalation of a phenyl ring. Heating $[Os_3(CO)_8(PFu_3)_2(\mu\text{-dppm})]$ at 110 °C gives $[Os_3(CO)_9(PFu_3)(\mu\text{-dppm})]$ together with the carbon-phosphorus bond cleavage products $[Os_3(CO)_7(\mu\text{-}PFu_2)(\mu_3\text{-}\eta^2\text{-}C_4H_2O)(\mu\text{-}H)(\mu\text{-dppm})]$ and $[Os_3(CO)_7(\mu\text{-}PFu_2)(\mu_3\text{-}\eta^2\text{-}C_6H_3CH_3)(\mu\text{-}H)(\mu\text{-dppm})]$. All new compounds were characterized by analytical and spectroscopic techniques together with single crystal X-ray diffraction analysis of nine clusters. Density functional theory (DFT) calculations have been carried out on isomers of $[Os_3(CO)_8(PR_3)_2(\mu\text{-dppm})]$ in order to understand the observed isomer ratios.

1. Introduction

The high reactivity associated with electronic and coordinative unsaturation in mononuclear transition metal complexes has been widely exploited in developing novel chemical behavior and in catalysis. In comparison, despite the widespread interest in cluster chemistry [1] the number of unsaturated low-valent clusters is extremely limited [2–14]. Amongst the most studied examples of electronically unsaturated clusters is $[Os_3(CO)_{10}(\mu\text{-}H)_2]$ [10], whose unsaturation derives from its 46e count. The diphosphine-substituted cluster $[Os_3(CO)_8\{\mu_3\text{-}Ph_2PCH_2P(Ph)C_6H_4\}(\mu\text{-}H)]$ (**1**) [11], first prepared by Smith and coworkers upon decarbonylation of $[Os_3(CO)_{10}(\mu\text{-dppm})]$, is not formally unsaturated but it behaves in this way as the relatively weak interaction of the orthometalated phenyl group with the triosmium center is easily removed. Consequently, **1** has been shown to have a rich chemistry [12,13], which is dominated by ligand addition rather than carbonyl substitution. For example, it undergoes facile and reversible carbonylation at 25 °C to afford saturated $[Os_3(CO)_9\{\mu_3\text{-}Ph_2PCH_2P(Ph)C_6H_4\}(\mu\text{-}H)]$ (**3**) which in turn adds further CO to regenerate the parent cluster **2** (Scheme 1) [11]. Recently, Hall, Richmond and coworkers have investigated these processes in some detail [14]. Their results show that carbonylation of **1** proceeds via an intermediate $[Os_3(CO)_8\{\mu\text{-}Ph_2PCH_2P(Ph)C_6H_4\}(\mu\text{-}H)]$ (**A**), in

* Corresponding authors.
E-mail address: skabir_ju@yahoo.com (S.E. Kabir).

0022-328X/$ – see front matter © 2013 Elsevier B.V. All rights reserved.
http://dx.doi.org/10.1016/j.jorganchem.2013.08.027

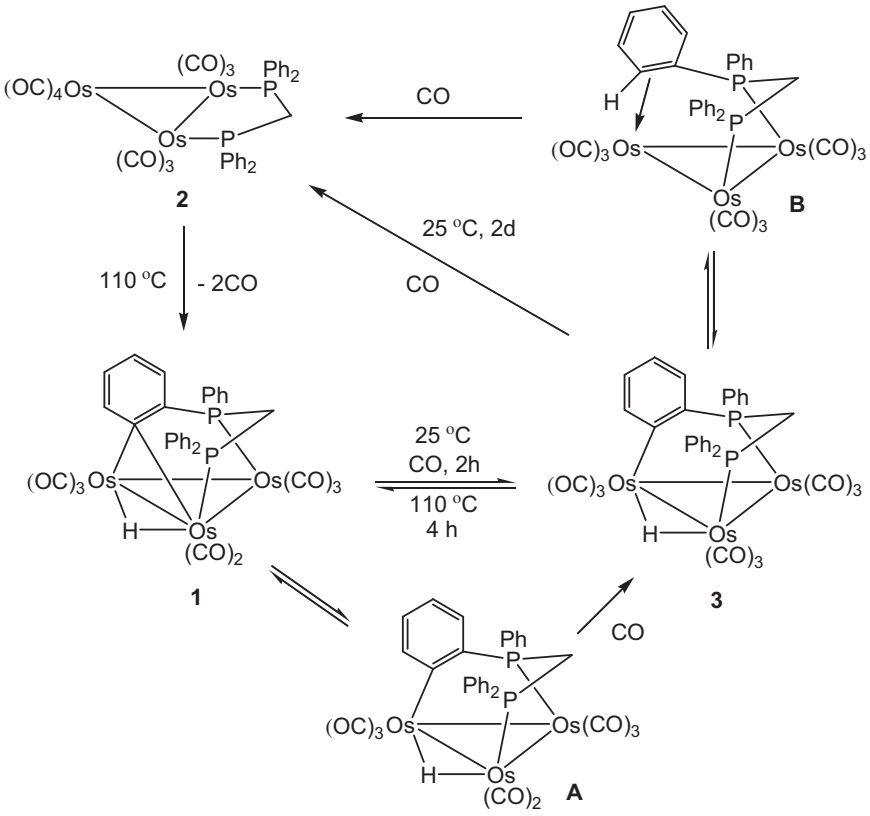

Scheme 1.

which an osmium-carbon bond involving the orthometalated phenyl moiety of the dppm ligand is broken, and a subsequent (rate-determining) associative step involving the addition of CO to the unsaturated intermediate, yielding $[Os_3(CO)_9\{\mu\text{-}Ph_2PCH_2P(Ph)C_6H_4\}(\mu\text{-}H)]$ (**3**). Further carbonylation of **3** then proceeds *via* a reductive coupling with formation of $[Os_3(CO)_9(\mu\text{-dppm})]$ (**B**) as an intermediate, a process which proceeds *via* an agostic intermediate, followed by two discrete π-aryl complexes (Scheme 1) [14].

Phosphines are widely used as ligands in transition metal-catalyzed reactions since they offer a wide variety of stereo-electronic properties that can substantially influence the course of a catalyzed reaction. One of the most widely utilized is triphenylphosphine which has been reported to react smoothly with **1** to afford $[Os_3(CO)_8(PPh_3)\{\mu_3\text{-}Ph_2PCH_2P(Ph)C_6H_4\}(\mu\text{-}H)]$ and $[Os_3(CO)_8(PPh_3)_2(\mu\text{-dppm})]$ [13d]. Over the past decade the chemistry of tri(2-furyl) phosphine (PFu_3) [15,16] and tri(2-thienyl)phosphine (PTh_3) [17] has been developed. Sterically they are akin to PPh_3; however, the electron-withdrawing nature of the 2-heteroaryl rings makes them poorer σ-donors than PPh_3 [17m]. This has been exploited in certain catalytic reactions, with PFu_3-containing catalysts often being more active than traditional PPh_3-based catalysts [16]. One aspect of our recent work has been a comparison of these three ligands in similar chemical systems [15c–f,17g–h] and herein we focus on an investigation of the comparative reactivity of the three phosphines towards lightly stabilized **1**.

2. Results and discussion

2.1. Reaction of $[Os_3(CO)_8\{\mu_3\text{-}Ph_2PCH_2P(Ph)C_6H_4\}(\mu\text{-}H)]$ (**1**) with PR_3 (R = Th, Fu, Ph)

Treatment of **1** with two equivalents of the requisite phosphine at 25 °C in dichloromethane gave four product types; $[Os_3(CO)_{10}(\mu\text{-dppm})]$ (**2**), $[Os_3(CO)_8(PR_3)\{\mu_3\text{-}Ph_2PCH_2P(Ph)C_6H_4\}(\mu\text{-}H)]$ (**4**–**6**), $[Os_3(CO)_9(PR_3)(\mu\text{-dppm})]$ (**7**–**9**) and $[Os_3(CO)_8(PR_3)_2(\mu\text{-dppm})]$ (**10**–**12**) (Scheme 2). Smith and coworkers previously reported that reaction of **1** with *ca.* one equivalent of PPh_3 gives **2**, **6** and **11**, while **9** has been prepared by Johnson, Lewis and coworkers from the reaction between $[Os_3(CO)_9(NCMe)(\mu\text{-dppm})]$ and PPh_3 [13d,18] Cluster **2** results from addition of two molecules of CO to **1**, with the CO presumably originating from cluster degradation. The characterization and mode of formation of each of the other product types is discussed separately in the following sections.

2.2. Phosphine addition products $[Os_3(CO)_8(PR_3)\{\mu_3\text{-}Ph_2PCH_2P(Ph)C_6H_4\}(\mu\text{-}H)]$ (**4**–**6**)

Clusters **4**–**6** are adducts of **1** and PR_3. The PPh_3 complex **6** has previously been spectroscopically characterized [13d] and data for **4** and **5** are similar. The $^{31}P\{^1H\}$ NMR spectrum of each displays a pair of doublets, assigned to the dppm ligand, and a singlet for the PR_3 ligand. The absence of coupling between the two phosphines suggests that either they are bound to different metal atoms or two phosphorus atoms bound to the same osmium lie *cis* to one another. Each cluster has a high field resonance in its ^1H NMR spectrum indicative of a bridging hydride (δ −18.1 for **4**; −18.4 for **5**; −15.9 for **6**). In order to fully elucidate the structures we have carried out an X-ray diffraction study of **5**, the results of which are summarized in Fig. 1. The structure of **5** is very similar to $[Os_3(CO)_8(PPr^i_3)\{\mu_3\text{-}Ph_2PCH_2P(Ph)C_6H_4\}(\mu\text{-}H)]$ [13d] and contains a triangle of osmium atoms with three distinct osmium–osmium bond distances [Os(1)—Os(2) 2.8961(6), Os(1)—Os(3) 2.8569(7) and Os(2)—Os(3) 3.0883(6) Å] the longest being spanned by the hydride (located and refined in the structural analysis). The PFu_3 ligand occupies an equatorial coordination site on Os(2), while the diphosphine is axially coordinated to Os(2) and Os(1) which

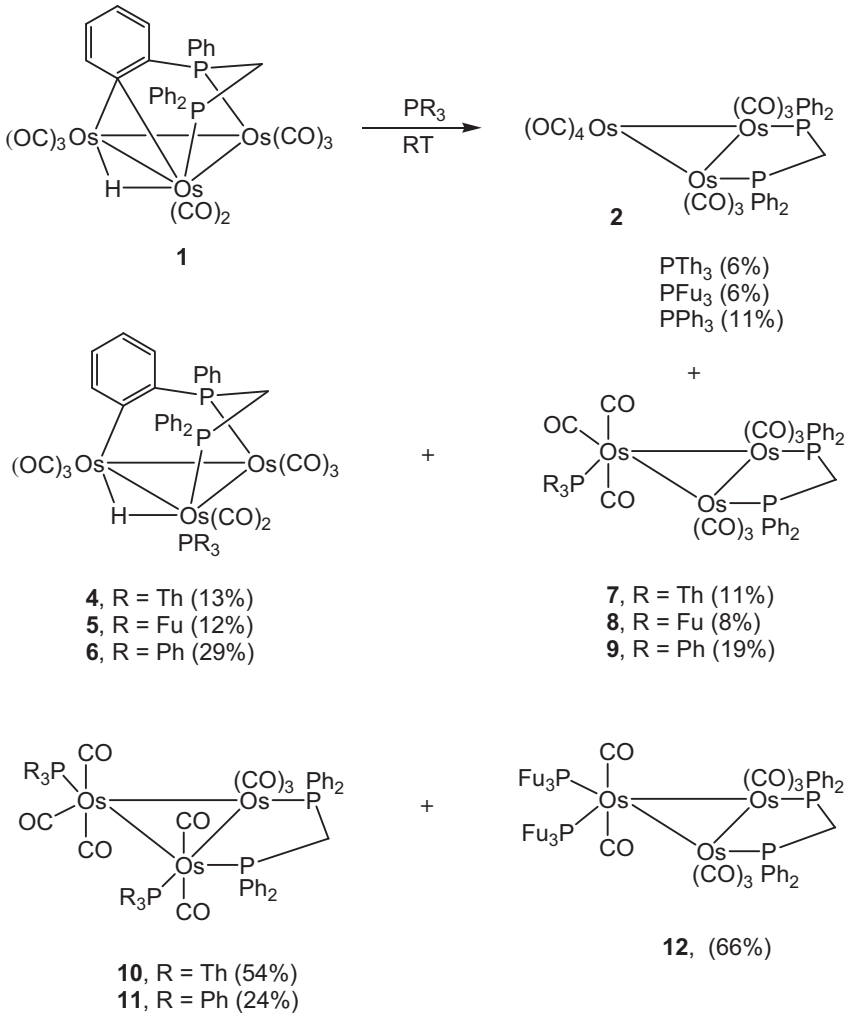

Scheme 2.

facilitates coordination of the C_6H_4 moiety to Os(3). The P(2)-Os(2)-P(3) bond angle of 94.96(6)o accounts for the lack of coupling between these phosphorus atoms. In $[Os_3(CO)_8(PPr^i_3)\{\mu_3\text{-}Ph_2PCH_2P(Ph)C_6H_4\}(\mu\text{-}H)]$, the osmium–phosphorus bonds sharing the same osmium atom [2.442(7) and 2.411(8) Å] are significantly longer than the third [2.334(8) Å] which Smith attributed to the extra electron-density on this osmium atom due to the presence of the PPr^i_3 ligand [13d]. In **5**, the osmium–phosphorus bond involving P(2) of the diphosphine ligand and Os(2) is significantly longer [2.427(2) Å] than the others [2.352(2) and 2.332(2) Å]. These differences may be a result of the better π-acceptor ability of PFu_3, while in contrast PPr^i_3 is a good σ-donor ligand. By analogy to the carbonylation of **1** that has been studied experimentally and computationally [14] (*vide supra*), it is likely that the phosphine adducts **4**–**6** are formed in a similar fashion to **3**; that is *via* the isomeric mono-metalated intermediate $[Os_3(CO)_8\{\mu\text{-}Ph_2PCH_2P(Ph)C_6H_4\}(\mu\text{-}H)]$ (**A**) (Scheme 1).

2.3. Phosphine and carbonyl addition products $[Os_3(CO)_9(PR_3)(\mu\text{-dppm})]$ (**7**–**9**)

Clusters **7**–**9** formally result from addition of both CO and phosphine to **1**, followed by carbon-hydrogen bond formation. The PPh_3 complex, **9**, has previously been reported by Johnson, Lewis and coworkers [18]. Spectroscopic data for **7**–**8** are in accord with that for **9** and also other complexes of the type $[Os_3(CO)_9L(\mu\text{-dppm})]$ [L = $P(OMe)_3$, $PHPh_2$] [18,19]. Each $^{31}P\{^1H\}$ NMR spectrum consists of a pair of doublets attributed to the diphosphine and a singlet for the monodentate phosphine, while all ^1H NMR spectra contain a triplet in the aliphatic region assigned to the methylene protons of the dppm ligand. We have determined the crystal structures of both **7** and **9**, which are shown in Figs. 2 and 3, respectively. Both are as expected; all phosphorus atoms lie in the equatorial plane and the gross structural features are similar to those of $[Os_3(CO)_9(PHPh_2)(\mu\text{-dppm})]$ [19] and $[Os_3(CO)_{10}(\mu\text{-dppm})]$ [20]. It seems likely that **7**–**9** result from the intermediate formation of **4**–**6**, followed by carbonyl addition, a process in which the monodentate phosphine also migrates to another osmium center. In a separate experiment we have shown that **6** reacts with CO to afford **9** as one of the products. This transformation is probably in competition with phosphine addition to **4**–**6** (see below), with the actual product distribution governed by the relative amounts of free CO and phosphine present in solution.

2.4. Double phosphine addition products $[Os_3(CO)_8(PR_3)_2(\mu\text{-dppm})]$ (**10**–**12**)

The fourth cluster type, and the major product in the case of all three phosphines, is $[Os_3(CO)_8(PR_3)_2(\mu\text{-dppm})]$ (**10**–**12**) which formally result from addition of two equivalents of phosphine to **1**

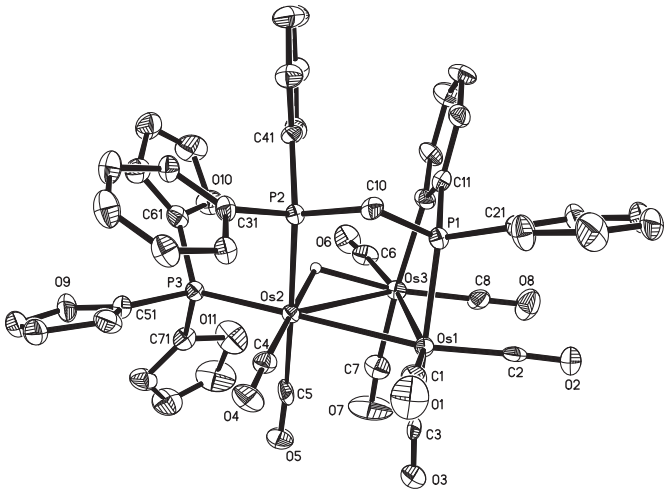

Fig. 1. ORTEP diagram of the molecular structure of $[Os_3(CO)_8(PFu_3)\{\mu_3\text{-}Ph_2PCH_2P(Ph)C_6H_4\}(\mu\text{-}H)]$ (**5**), showing 50% probability thermal ellipsoids. Ring hydrogen atoms are omitted for clarity. Selected bond distances (Å) and angles(°): Os(1)—Os(2) 2.8961(6), Os(1)—Os(3) 2.8569(7), Os(2)—Os(3) 3.0883(6), Os(1)—P(1) 2.352(2), Os(2)—P(2) 2.4267(19), Os(2)—P(3) 2.3316(18), Os(3)—Os(1)—Os(2) 64.931(10), Os(1)—Os(2)—Os(3) 56.921(15), Os(1)—Os(3)—Os(3) 58.148(15), P(3)—Os(2)—Os(3) 111.81(5), C(4)—Os(2)—P(3) 101.1(2), P(3)—Os(2)—P(2) 94.96(6), P(1)—Os(1)—Os(3) 85.32(5), P(1)—Os(1)—Os(2) 86.81(5), C(6)—Os(3)—C(12) 89.2(3), C(12)—Os(3)—Os(1) 91.6(2), P(1)—C(10)—P(2) 107.5(4).

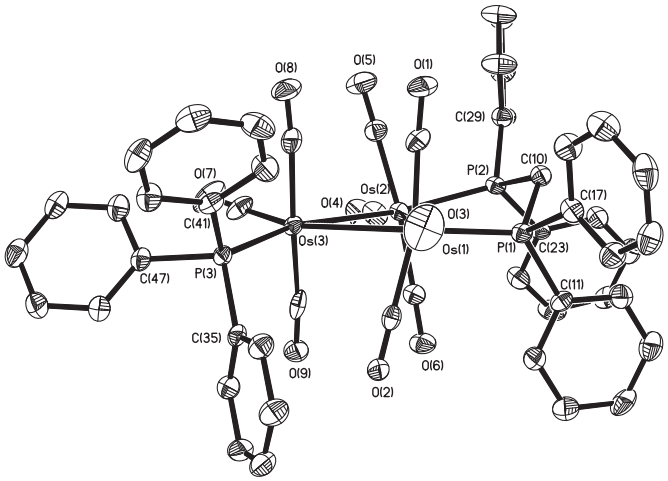

Fig. 3. ORTEP diagram of the molecular structure of $[Os_3(CO)_9(PPh_3)(\mu\text{-dppm})]$ (**9**), showing 50% probability thermal ellipsoids. Ring hydrogen atoms are omitted for clarity. Selected bond distances (Å) and angles(°): Os(1)—Os(2) 2.8768(4), Os(1)—Os(3) 2.9149(5), Os(2)—Os(3) 2.8871(4), Os(1)—P(1) 2.3349(11), Os(2)—P(2) 2.3311(11), Os(3)—P(3) 2.3560(11), Os(2)—Os(1)—Os(3) 59.796(6), Os(1)—Os(2)—Os(3) 60.757(10), Os(2)—Os(3)—Os(1) 59.447(10), P(3)—Os(3)—Os(1) 102.82(3), P(3)—Os(3)—Os(2) 160.89(3), C(7)—Os(3)—P(3) 99.94(15), C(8)—Os(3)—P(3) 90.84(15), P(1)—C(10)—P(2) 112.1(2).

with concomitant carbon–hydrogen bond formation. Two isomeric forms are seen (Chart 1), and these are denoted as the 1,1- and 1,2-isomer. Smith and coworkers previously found that PPh_3 afforded only the 1,2-isomer, whereas other phosphines and phosphites gave the 1,1-isomer [13d]. With $P(OMe)_3$ both isomers were formed and could be separated by TLC, and the X-ray structure of the 1,1-isomer was reported. The same authors also reported the X-ray structure of 1,2-$[Os_3(CO)_8(PPh_3)_2(\mu\text{-dppm})]$ (**11**) [13d] and we have previously shown that $[Os_3(CO)_8(PHPh_2)_2(\mu\text{-dppm})]$ is a 1,1-isomer [19]. In order to confirm the nature of the different isomers, we

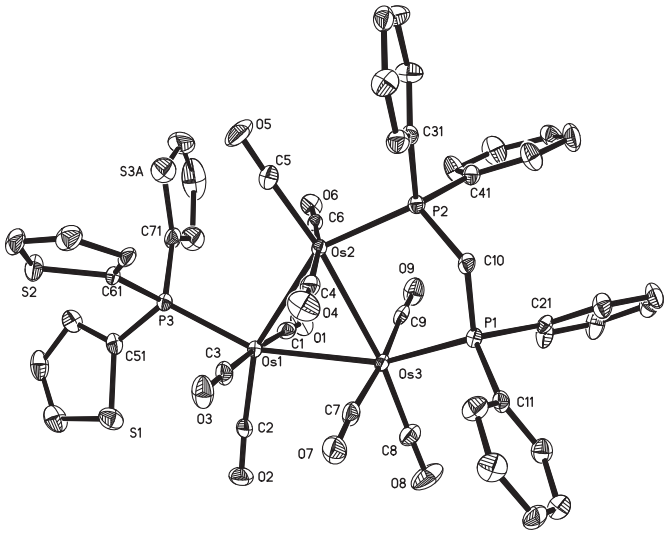

Fig. 2. ORTEP diagram of the molecular structure of $[Os_3(CO)_9(PTh_3)(\mu\text{-dppm})]$ (**7**), showing 50% probability thermal ellipsoids. Ring hydrogen atoms are omitted for clarity. Selected bond distances (Å) and angles(°): Os(1)—Os(2) 2.9141(4), Os(1)—Os(3) 2.8829(3), Os(2)—Os(3) 2.8856(4), Os(1)—P(3) 2.3345(12), Os(2)—P(2) 2.3370(11), Os(3)—P(1) 2.3242(11), Os(3)—Os(1)—Os(2) 59.703(8), Os(3)—Os(2)—Os(1) 59.610(6), Os(1)—Os(3)—Os(3) 60.687(9), P(3)—Os(1)—Os(2) 100.42(3), P(3)—Os(1)—Os(3) 159.03(3), C(2)—Os(1)—P(3) 104.26(15), C(1)—Os(1)—P(3) 91.30(14), P(1)—C(10)—P(2) 111.6(2).

have determined the crystal structures of **10** and **12**, the results of which are shown in Figs. 4 and 5, respectively. For **10** there are two independent triosmium clusters (and three molecules of dichloromethane) in the asymmetric unit.

In the solid state, **10** exists as the 1,2-isomer while **12** is a 1,1-isomer. Akin to the situation for **11**, $[Os_3(CO)_8\{P(OMe)_3\}_2(\mu\text{-dppm})]$ [13d] and $[Os_3(CO)_8(PHPh_2)_2(\mu\text{-dppm})]$ [19], all phosphorus atoms in both **10** and **12** occupy equatorial coordination sites. Spectroscopic data for non-crystalline samples of **10** showed the presence of both isomers in solution (Scheme 3). Thus, the $^{31}P\{^1H\}$ NMR spectrum displays two sets of resonances in an approximate 5:1 ratio. The 1,2-isomer (**10a**) is the major form characterized by signals at −20.7 (dd, J_{PP} = 50.2, 9.2 Hz), −27.3 (d, J_{PP} = 50.2 Hz), −39.3 (d, J_{PP} = 9.2 Hz) and −51.8 (s) ppm due to the four non-equivalent phosphorus atoms, while the minor 1,1-isomer (**10b**) appears as two singlets at −29.1 and −40.8 ppm. In contrast, spectroscopic data for **12** show that only the solid-state structure (1,1-isomer) exists in solution, being observed as two equal intensity singlets. We have carried out VT NMR studies of both **10** and **11** in d_8-toluene. No significant changes were seen in the ^{31}P NMR spectrum of 1,2-$[Os_3(CO)_8(PPh_3)_2(\mu\text{-dppm})]$ (**11**) upon warming to 80 °C. Above this temperature, the bright yellow solution lightened and a number of new resonances appeared due to irreversible changes resulting from loss of PPh_3 (see following section). Heating a sample of pure 1,2-$[Os_3(CO)_8(PTh_3)_2(\mu\text{-dppm})]$ (**10a**) to 80 °C led to no significant change; however, between 80 and 100 °C, the disappearance of **10a** was observed with concomitant formation of the 1,1-isomer **10b**. Scheme 3 illustrates this transformation. Maintaining this sample at 100 °C for several hours led to the appearance of a number of new resonances associated with phosphine loss and secondary rearrangement products (see following section).

In order to further probe the relative stability of 1,1- and 1,2-isomers of **10**–**12**, we have performed density functional theory (DFT) calculations on both sets of isomers. Fig. 6 shows the optimized structures for **10a** and **10b**, where the 1,2-isomer is 4.8 kcal/mol lower in energy than the 1,1-isomer. The ligand disposition in the optimized structure of **10a** agrees nicely with the solid-state structure that is exhibited in Fig. 4. On the basis of the

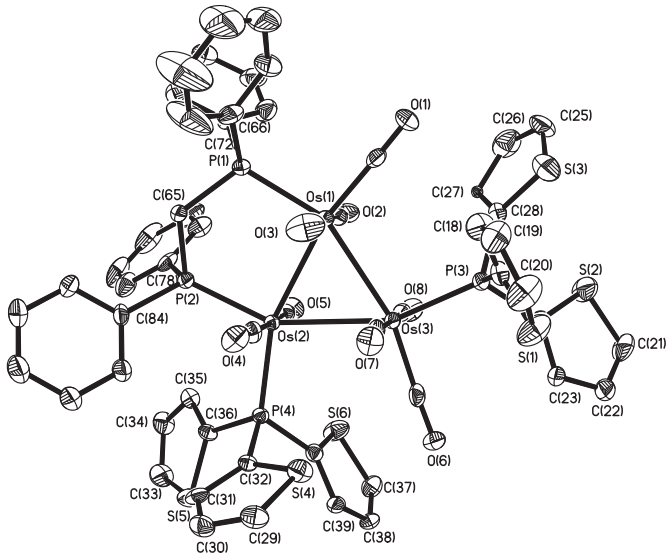

Fig. 4. ORTEP diagram of the molecular structure of one of the unique molecules of $[Os_3(CO)_8(PTh_3)_2(\mu\text{-dppm})]$ (**10**), showing 50% probability thermal ellipsoids. Ring hydrogen atoms are omitted for clarity. Selected bond distances (Å) and angles(°): Os(1)—Os(2) 2.8882(4), Os(1)—Os(3) 2.9128(5), Os(2)—Os(3) 2.9112(4), Os(1)—P(1) 2.3269(17), Os(2)—P(2) 2.3170(16), Os(3)—P(3) 2.3196(17), Os(2)—P(4) 2.3091(16), Os(2)—Os(1)—Os(3) 60.242(8), Os(1)—Os(2)—Os(3) 60.298(11), Os(2)—Os(3)—Os(1) 59.461(11), P(3)—Os(3)—Os(1) 97.51(4), P(3)—Os(3)—Os(2) 156.97(4), C(7)—Os(3)—P(3) 92.1(2), P(4)—Os(2)—P(2) 108.09(6), C(4)—Os(2)—P(4) 92.1(2), P(4)—Os(2)—Os(1) 159.42(4), P(4)—Os(2)—Os(3) 99.53(4), P(1)—C(65)—P(2) 116.7(3).

free-energy difference between **10a** and **10b**, a K_{eq} value of 3×10^{-4} is computed, and this is in concert with the experimental data and the observation of only **10a** in the initial synthesis. While heating **10a** furnishes **10b** through the formal migration of a single PTh_3 ligand about the cluster polyhedron, the mechanism by which the thermodynamically less stable isomer **10b** forms is far from clear. We have kinetically and computationally investigated the isomerization behavior of related phosphines at $Os_3(CO)_{10}(PP)$ clusters (where PP = diphosphine) [21]. In these examples, the isomerization was well-behaved and does not involve the dissociation of the diphosphine ligand from the cluster. In the case of the $Os_3(CO)_8(PR_3)_2(dppm)$ clusters investigated in this study, no attempt has been made to study this isomerization process by DFT because of the complexity of the reaction which is likely to proceed *via* the loss of a monodentate PR_3 ligand, followed by ligand capture at the putative unsaturated cluster $Os_3(CO)_8(PR_3)(dppm)$.

The geometry of cluster **12** was subjected to DFT analysis and the optimized structure (not shown) was consistent with the solid-structure structure. The corresponding 1,2-isomer based on **12** was also optimized and the disposition of the ancillary ligands about the cluster polyhedron paralleled the DFT structure computed for **10a**. The energy difference for the two PFu_3-based clusters is small (ΔG = 0.8 kcal/mol) and favors that of the crystallographically observed isomer. While the ground-state energy difference between the two isomers is small, the activation barrier is assuredly much greater and no equilibration of the two isomers is expected at room temperature.

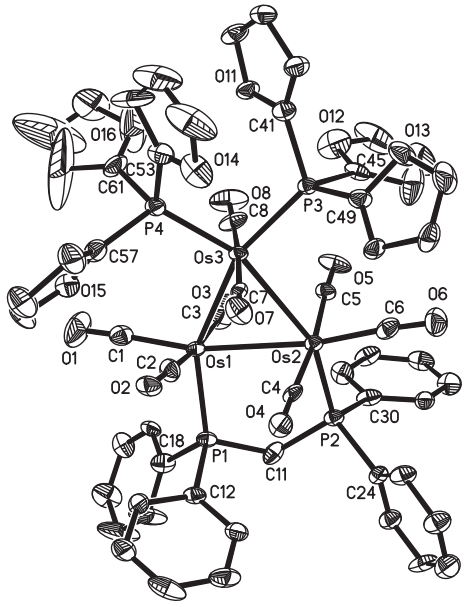

Fig. 5. ORTEP diagram of the molecular structure of $[Os_3(CO)_8(PFu_3)_2(\mu\text{-dppm})]$ (**12**), showing 50% probability thermal ellipsoids. Ring hydrogen atoms are omitted for clarity. Selected bond distances (Å) and angles(°): Os(1)—Os(2) 2.8732(5), Os(1)—Os(3) 2.8960(5), Os(2)—Os(3) 2.8942(6), Os(1)—P(1) 2.304(2), Os(2)—P(2) 2.308(2), Os(3)—P(3) 2.282(2), Os(3)—P(4) 2.281(2), Os(2)—Os(1)—Os(3) 60.220(14), Os(1)—Os(2)—Os(3) 60.281(11), Os(2)—Os(3)—Os(1) 59.499(13), P(3)—Os(3)—Os(1) 154.15(6), P(3)—Os(3)—Os(2) 97.96(6), C(7)—Os(3)—P(3) 99.94(15), C(8)—Os(3)—P(3) 90.1(3), C(7)—Os(3)—P(4) 86.7(2), P(1)—C(11)—P(2) 116.9(5).

2.5. Thermolysis of $[Os_3(CO)_8(PR_3)_2(\mu\text{-dppm})]$ (**10**–**11**): phosphine loss and carbon–hydrogen bond activation

From the variable temperature (VT) NMR studies discussed above, we were aware that the bis(phosphine) complexes **10**–**11** were unstable at higher temperatures. In order to probe this behavior, we heated **10**–**11** independently in toluene which furnished two products in each case (Scheme 4). The major product found in both reactions was $[Os_3(CO)_9(PR_3)(\mu\text{-dppm})]$ (**7** and **9**), resulting from phosphine substitution by CO, while the second products were the new lightly stabilized clusters $[Os_3(CO)_7(PR_3)\{\mu_3\text{-}Ph_2PCH_2P(Ph)C_6H_4\}(\mu\text{-H})]$ (**13**–**14**), which are formed upon loss of both phosphine and CO with concomitant oxidative addition of a carbon-hydrogen bond.

The molecular structures of **13** and **14** are shown in Figs. 7 and 8, respectively, with the captions containing selected bond lengths and angles. The overall structures are very similar to that of **1** apart from the replacement of an equatorial carbonyl group of **1** by a phosphine ligand. As in **1**, the osmium–osmium edge that is simultaneously bridged by the metalated phenyl group and the hydride ligand [2.747(1) Å in **1**; 2.7732(7) Å in **13** and 2.7729(7) Å in **14**] is significantly shorter than the other two [2.844(1) and 2.834(1) Å in **1**; 2.8415(7) and 2.8455(8) Å in **13**; 2.8492(6) and 2.8470(6) Å in **14**], a condition that reflects the constraining influence to the two bridging ligands. The most notable feature of **13** and **14** is the position of the phosphine ligand that is bound to the osmium atom that is not coordinated by the diphosphine. Spectroscopic data are consistent with the solid-state structures. Each $^{31}P\{^1H\}$ NMR spectrum consists of two doublets and a singlet in 1:1:1 ratio, as expected for the three non-equivalent phosphorus atoms in the cluster, and the hydride resonance in the ^1H NMR spectra appears as a doublet of doublet of doublets. Clusters **13** and **14** are CO substitution products of **1** that are not formed from the direct reaction of **1** with these phosphines (Scheme 1). This underscores the difference in reactivity between electronically saturated and unsaturated carbonyl clusters; the former being dominated by CO substitution.

The mode of formation of these products (Scheme 4) is not fully understood, however, given the very similar outcomes of the two reactions we assume that they take place by the same mechanism. For **10,** we know from VT NMR studies (see preceding section) that heating at 100 °C promotes the formation of the 1,1-isomer

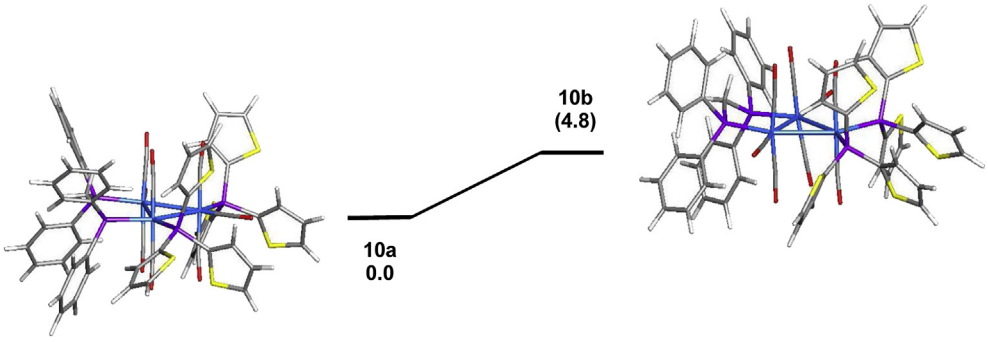

Fig. 6. Geometry-optimized structures for the isomeric clusters **10a** and **10b**. The quoted free-energy (kcal/mol) difference is relative to **10a** at room temperature.

10b (Scheme 3). While we cannot show this for **11**, we assume that isomerization also occurs but under the conditions required to facilitate this, secondary processes leading to formation of **9** and **14** are competitive. Loss of a phosphine from the 1,1-isomers would result in the unsaturated intermediates, $[Os_3(CO)_8(PR_3)(\mu\text{-dppm})]$, which can add CO to give **7** and **9** or undergo C–H activation, followed by CO loss, to give **13** and **14**. Hall and Richmond [14] have recently shown that addition of CO to the intermediate 46-electron cluster $[Os_3(CO)_9(\mu\text{-dppm})]$ (**B**) (Scheme 1) is rapid, and it seems reasonable to suggest that the same is true for the putative species $[Os_3(CO)_8(PR_3)(\mu\text{-dppm})]$. The added CO must result from another cluster molecule, which, in turn, has undergone C–H activation.

2.6. Thermolysis of $[Os_3(CO)_8(PFu_3)_2(\mu\text{-dppm})]$ (**12**): carbon–phosphorus bond cleavage

Heating **12** in toluene for 2 h followed a different course to that of **10**–**11**, leading instead to the formation of three products; $[Os_3(CO)_9(PFu_3)(\mu\text{-dppm})]$ (**8**) (19%), $[Os_3(CO)_7(\mu\text{-PFu}_2)(\mu_3\text{-}\eta^2\text{-}C_4H_2O)(\mu\text{-H})(\mu\text{-dppm})]$ (**15**) (40%) and $[Os_3(CO)_7(\mu\text{-PFu}_2)(\mu_3\text{-}\eta^2\text{-}C_6H_3CH_3)(\mu\text{-H})(\mu\text{-dppm})]$ (**16**) (31%) (Scheme 5). Cluster **8** results from phosphine substitution by CO, while cluster **15** results from a loss of one PFu_3 ligand, coupled with the activation of one carbon-phosphorus bond in remaining the PFu_3 ligand. This P–C bond cleavage generates the observed phosphido and capping furyne ($\mu_3\text{-}\eta^2\text{-}C_4H_2O$) groups in the product. The isolation of cluster **16** provides evidence for the activation of the toluene solvent during the thermolysis reaction. An independent control experiment has confirmed that the furyne cluster **15** does not serve as a precursor to **16**.

ORTEP diagrams of the molecular structures of **15** and **16** are depicted in Figs. 9 and 10, and selected bond distances and angles are listed in the captions. Both are similar to the triruthenium thiophyne and furyne clusters $[Ru_3(CO)_7\{\mu\text{-P}(C_4H_3E)_2\}(\mu_3\text{-}\eta^2\text{-}C_4H_2E)(\mu\text{-H})(\mu\text{-dppm})]$ (E = S, O) [17b]. A $\mu_3\text{-}\eta^2\text{-}C_4H_2O$ (in **15**) and $\mu_3\text{-}\eta^2\text{-}C_6H_3CH_3$ (in **16**) ligand caps the open triangular array of osmium atoms. The hydride was not located directly but it is believed to span the dppm-bridged edge due to the significant lengthening of this bond [Os(2)—Os(3) 2.9668(4) Å in **15**; Os(1)—Os(2) 2.9494(7) Å in **16**] as compared to the other [Os(1)—Os(2) 2.8508(4) Å in **15**; Os(2)—Os(3) 2.8527(6) Å in **16**]. In both, the phosphido group bridges the open edge of the cluster in a slightly unsymmetrical fashion [Os(1)—P(1) 2.396(2) and Os(3)—P(1) 2.373(2) Å in **15**; Os(3)—P(3) 2.393(2) and Os(1)—P(3) 2.364(2) Å in

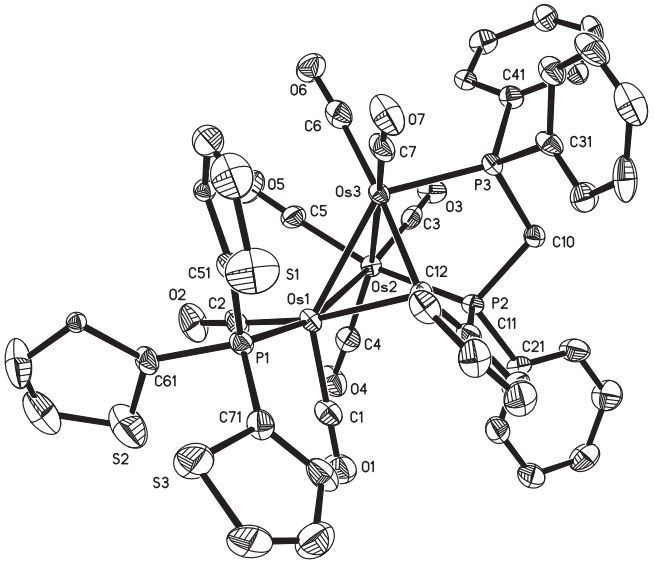

Fig. 7. ORTEP diagram of the molecular structure of $[Os_3(CO)_7(PTh_3)\{\mu_3\text{-}Ph_2PCH_2P(Ph)C_6H_4\}(\mu\text{-H})]$ (**13**), showing 50% probability thermal ellipsoids. Ring hydrogen atoms are omitted for clarity. Selected bond distances (Å) and angles(°): Os(1)—Os(2) 2.8415(7), Os(1)—Os(3) 2.7732(7), Os(2)—Os(3) 2.8455(8), Os(1)—P(1) 2.360(2), Os(2)—P(2) 2.336(2), Os(3)—P(3) 2.325(2), Os(1)—C(12) 2.362(8), Os(3)—C(12) 2.238(8), Os(3)—Os(1)—Os(2) 60.886(16), Os(1)—Os(2)—Os(3) 58.372(11), Os(1)—Os(3)—Os(2) 60.742(19), P(1)—Os(1)—Os(3) 110.02(5), P(1)—Os(1)—Os(2) 166.33(5), P(2)—Os(2)—Os(3) 77.98(5), P(2)—Os(2)—Os(1) 85.67(5), P(3)—Os(3)—Os(1) 131.33(5), P(3)—Os(3)—Os(2) 89.25(5), Os(3)—C(12)—Os(1) 74.1(2), C(2)—Os(1)—Os(3) 116.6(3), C(6)—Os(3)—Os(1) 121.3(3), P(2)—C(10)—P(3) 107.3(4).

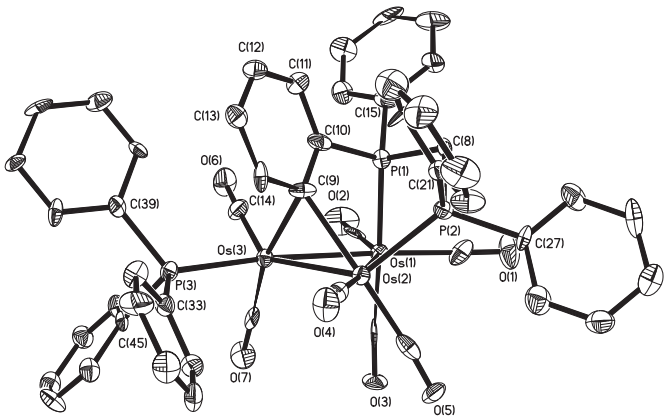

Fig. 8. ORTEP diagram of the molecular structure of $[Os_3(CO)_7(PPh_3)\{\mu_3\text{-}Ph_2PCH_2P(Ph)C_6H_4\}(\mu\text{-H})]$ (**14**), showing 50% probability thermal ellipsoids. Ring hydrogen atoms are omitted for clarity. Selected bond distances (Å) and angles(°): Os(1)—Os(2) 2.8492(6), Os(1)—Os(3) 2.8470(6), Os(2)—Os(3) 2.7729(7), Os(1)—P(1) 2.331(2), Os(2)—P(2) 2.324(2), Os(3)—P(3) 2.372(2), Os(2)—C(9) 2.245(9), Os(3)—C(9) 2.430(9), Os(3)—Os(1)—Os(2) 58.260(16), Os(3)—Os(2)—Os(1) 60.830(14), Os(2)—Os(3)—Os(1) 60.910(15), P(3)—Os(3)—Os(1) 172.19(6), P(3)—Os(3)—Os(2) 111.99(6), P(1)—Os(1)—Os(3) 84.54(6), P(1)—Os(1)—Os(2) 77.36(6), P(2)—Os(2)—Os(3) 131.01(6), P(2)—Os(2)—Os(1) 90.03(6), Os(2)—C(9)—Os(3) 72.6(2), C(5)—Os(2)—Os(3) 117.7(3), C(7)—Os(3)—Os(2) 114.9(3), P(1)—C(8)—P(2) 107.9(4).

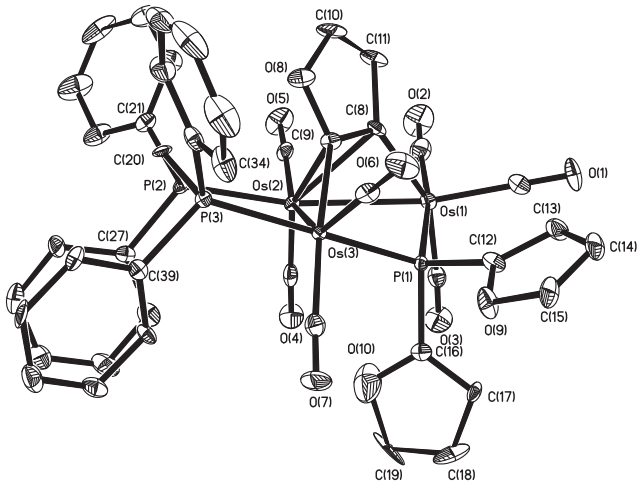

Fig. 9. ORTEP diagram of the molecular structure of $[Os_3(CO)_7(\mu\text{-}PFu_2)(\mu_3\text{-}\eta^2\text{-}C_4H_2O)(\mu\text{-}H)(\mu\text{-}dppm)]$ (**15**), showing 50% probability thermal ellipsoids. Ring hydrogen atoms are omitted for clarity. Selected bond distances (Å) and angles(°): Os(1)—Os(2) 2.8508(4), Os(2)—Os(3) 2.9668(4), Os(1)—P(1) 2.3956(17), Os(2)—P(2) 2.3534(17), Os(3)—P(3) 2.3750(16), Os(3)—P(1) 2.3734(16), Os(1)—C(8) 2.119(7), Os(3)—C(9) 2.125(6), Os(2)—C(8) 2.427(6), Os(2)—C(9) 2.282(6), Os(1)—Os(2)—Os(3) 84.723(10), P(1)—Os(3)—P(3) 169.29(6), P(1)—Os(3)—Os(2) 76.45(4), P(1)—Os(1)—Os(2) 78.47(4), Os(3)—P(1)—Os(1) 110.60(6), Os(3)—C(9)—Os(2) 84.5(2), Os(1)—C(8)—Os(2) 77.3(2), C(9)—Os(2)—C(8) 34.2(2), C(6)—Os(3)—Os(2) 140.03(19), C(4)—Os(2)—Os(3) 114.7(2), P(2)—C(20)—P(3) 113.6(3).

16]. Each capping ligand is bound to the cluster through a η^2,π-interaction, being slightly tilted toward the π-coordination side as observed in the related thiophyne clusters $[Os_3(CO)_9(\mu_3\text{-}\kappa^1\text{:}\eta^2\text{-}PTh_2(C_4H_2S)(\mu\text{-}H)]$ [17g], $[Os_3(CO)_9(\mu_3\text{-}\kappa^1\text{:}\eta^2\text{-}PPh_2(C_4H_2S)(\mu\text{-}H)]$ [17d] and $[Os_3(CO)_8(PPh_2Th)\{\mu_3\text{-}\kappa^1\text{:}\eta^2\text{-}PTh_2(C_4H_2S)\}(\mu\text{-}H)]$ [17d].

Spectroscopic data support the observed solid-state structures, for example ESI mass spectra show $[M^+-H]$ peaks at m/z 1383 (for

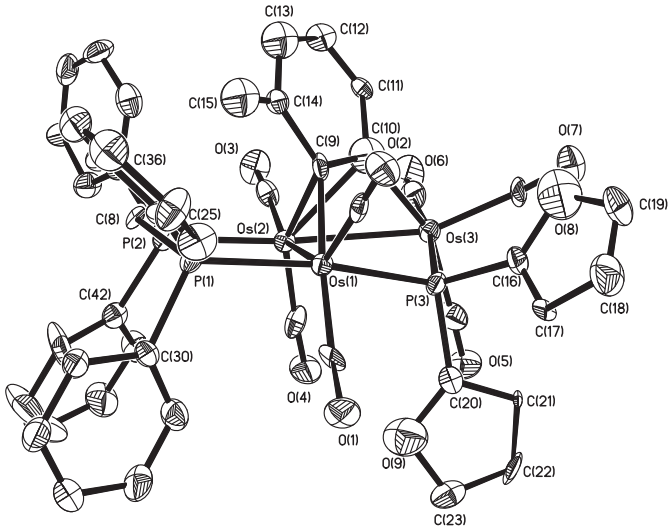

Fig. 10. ORTEP diagram of the molecular structure of one of the unique molecules of $[Os_3(CO)_7(\mu\text{-}PFu_2)(\mu_3\text{-}\eta^2\text{-}C_6H_3CH_3)(\mu\text{-}H)(\mu\text{-}dppm)]$ (**16**), showing 50% probability thermal ellipsoids. Ring hydrogen atoms are omitted for clarity. Selected bond distances (Å) and angles(°): Os(1)—Os(2) 2.9494(7), Os(2)—Os(3) 2.8527(6), Os(1)—P(1) 2.391(2), Os(2)—P(2) 2.366(2), Os(3)—P(3) 2.393(2), Os(1)—P(3) 2.364(2), Os(1)—C(9) 2.169(10), Os(2)—C(10) 2.329(9), Os(2)—C(9) 2.243(9), Os(3)—C(10) 2.093(9), Os(3)—Os(2)—Os(1) 83.803(14), P(3)—Os(1)—P(1) 167.87(8), P(3)—Os(1)—Os(2) 80.03(6), P(3)—Os(3)—Os(2) 81.61(5), Os(1)—P(3)—Os(3) 109.15(9), Os(1)—C(9)—Os(2) 83.9(3), Os(3)—C(10)—Os(2) 80.2(3), C(9)—Os(2)—C(10) 37.0(3), C(1)—Os(1)—Os(2) 130.6(3), C(4)—Os(2)—Os(1) 110.2(3), P(1)—C(8)—P(2) 114.8(4).

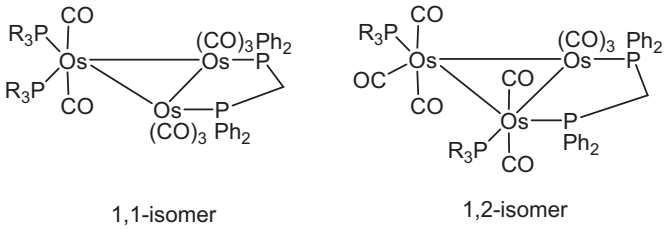

Chart 1.

15) and 1411 (for **16**) associated with the molecular ions. NMR spectra of **15** show that in solution it exists in two isomeric forms. Thus, the $^{31}P\{^1H\}$ NMR spectrum consists of two sets of resonances in 4:1 ratio, each set consisting of two doublets and a doublet of doublet due to the three phosphorus atoms. Consistent with this, the aliphatic region of the ^1H NMR spectrum exhibits four resonances for the methylene protons of the dppm ligand at δ 3.34, 3.10, 2.73, and 2.53 with a relative intensity of 4:1:1:4, respectively, while the hydride region displays two multiplets at δ −17.31 and −17.27 also in a 4:1 ratio. We have observed similar isomerization of furyne clusters previously [15i] and it most likely arises from the different relative orientations of the oxygen atom in the furyne ring (Chart 2). For **16**, the spectroscopic data are in agreement with the solid-state structure. The ^1H NMR spectrum reveals twenty-nine aromatic hydrogens as series of multiplets from δ 6.32–7.62, with the lone methyl group appearing as a singlet at δ 1.57. The diastereotopic methylene hydrogens and the bridging hydride appear as separate resonances centered at δ 3.26, 2.50, and −17.22, respectively. The ^{31}P NMR and ESI mass spectral data are summarized in the experimental section.

3. Summary and conclusions

In this work we set out to investigate the comparative reactivity of PTh_3, PFu_3 and PPh_3 towards the lightly stabilized triosmium cluster $[Os_3(CO)_8\{\mu_3\text{-}Ph_2PCH_2P(Ph)C_6H_4\}(\mu\text{-}H)]$ (**1**). As detailed in Scheme 2, even at room temperature the reaction is complex and leads to a number of different product types. The three phosphines broadly behave in a similar manner, although it is notable that PTh_3 and PFu_3 favor formation of the bis(phosphine) adducts $[Os_3(CO)_8(PR_3)_2(\mu\text{-}dppm)]$ **10** (54%) and **12** (66%) respectively, while with PPh_3 products **6** and **9** (29 and 19%) containing a single phosphine ligand are more abundant. The key intermediates in determining this product ratio are likely the saturated monophosphine complexes $[Os_3(CO)_8(PR_3)\{\mu_3\text{-}Ph_2PCH_2P(Ph)C_6H_4\}(\mu\text{-}H)]$ (**4**–**6**). For both PFu_3 and PTh_3 the major products are the bis(phosphine) complexes $[Os_3(CO)_8(PR_3)_2(\mu\text{-}dppm)]$ (**10** and **12**), further phosphine addition being favored with respect to PPh_3 by both their smaller cone angles (PFu_3 133° vs PPh_3 148°) and the stronger π-acceptor nature, which reduces electron-density at the cluster center. Both 1,1- and 1,2-isomers were found, and in order to probe their relative stabilities a series of DFT calculations were carried out, and the computed free energies (at room temperature) of the different isomers are in agreement with the experimentally observed diffraction structures. The bis(phosphine) complexes were not stable at higher temperatures and converted into a number of new species, all of which resulted from phosphine loss. Interestingly, while PPh_3 and PTh_3 complexes **10**–**11** behaved in a similar manner, thermal rearrangement cleavage of the PFu_3 adduct **12** was dominated by carbon–phosphorus bond cleavage of the PFu_3 ligand (71% total yield). This resulted in formation of a new furyne cluster **15** together with a related toluene-derived complex **16**, formally resulting from exchange of the furyne by the reaction solvent.

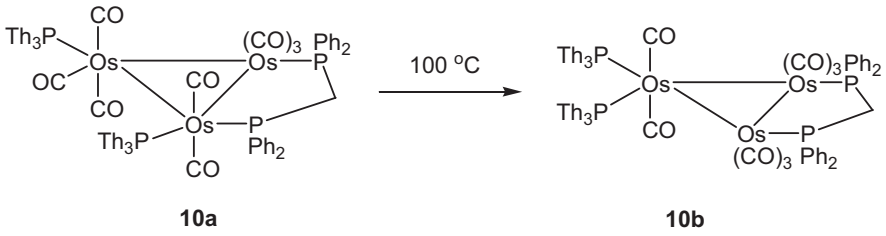

10a **10b**

Scheme 3.

This work demonstrates that the relatively simple procedure of adding two equivalents of a phosphine to **1** is considerably more complicated than expected, and further that there are some significant differences not only between PPh_3 and PFu_3/PTh_3 but also between PFu_3 and PTh_3. This mirrors many aspects of our previous work with these phosphines [15c–f,17g–h] and suggests that the chemistries of these ligands are significantly different warranting further study.

4. Experimental

4.1. General

$[Os_3(CO)_{12}]$ was purchased from Strem Chemicals Inc. and used without further purification and $[Os_3(CO)_8\{\mu_3\text{-}Ph_2PCH_2P(Ph)C_6H_4\}(\mu\text{-}H)]$ (**1**) was prepared according to the published procedure [11]. Triphenylphosphine, tri(2-thienyl)phosphine and tri(2-furyl) phosphine were purchased from *E.* Merck, Acros Organics and Aldrich, respectively, and used as received. All reactions were carried out under a nitrogen atmosphere using standard Schlenk techniques. Reagent-grade solvents were dried by standard methods prior to use. Infrared spectra were recorded on a Shimadzu FTIR 8101 spectrophotometer. NMR spectra were recorded on Bruker DPX 400 instruments. Elemental analyses were performed by Microanalytical Laboratories, University College London.

4.2. Reaction of $[Os_3(CO)_8\{\mu_3\text{-}Ph_2PCH_2P(Ph)C_6H_4\}(\mu\text{-}H)]$ (**1**) with PTh_3

To a CH_2Cl_2 solution (20 mL) of **1** (50 mg, 0.042 mmol) was added PTh_3 (24 mg, 0.086 mmol) and the mixture was then stirred at 25 °C for 8 h. The solvent was removed by rotary evaporation and the residue chromatographed by TLC on silica gel. Elution with hexane/CH_2Cl_2 (7:3, v/v) gave four bands which afforded the following compounds in order of elution: $[Os_3(CO)_{10}(\mu\text{-dppm})]$ (**2**) (3 mg, 6%) as yellow crystals, $[Os_3(CO)_8(PTh_3)\{\mu_3\text{-}Ph_2PCH_2P(Ph)C_6H_4\}(\mu\text{-}H)]$ (**4**) (8 mg, 13%) as yellow crystals, $[Os_3(CO)_9(PTh_3)(\mu\text{-dppm})]$ (**7**) (7 mg, 11%) as yellow crystals and $[Os_3(CO)_8(PTh_3)_2(\mu\text{-dppm})]$ (**10**) (40 mg, 54%) as orange crystals after recrystallization from hexane/CH_2Cl_2 at 4 °C. Characterizing data for **4**: Anal. Calcd for $C_{45}H_{31}O_8Os_3P_3S_3$: C, 37.03; H, 2.14. Found: C, 37.29; H, 2.19. IR (CH_2Cl_2): ν_{CO} = 2025 m, 2001 vs, 1987 s, 1949 m, 1932 m, br cm^{-1}. ^1H NMR ($CDCl_3$, 25 °C): δ = 8.54 (m, 2H), 8.24 (m, 2H), 7.67 (m, 15H), 7.09 (m, 2H), 6.96 (m, 2H), 6.79 (m, 1H), 6.43 (m, 2H), 6.14 (m, 1H), 5.90 (m, 1H), 5.24 (m, 1H), 3.82 (m, 1H), −18.09 (m, 1H). $^{31}P\{^1H\}$ NMR ($CDCl_3$, 25 °C): δ = −40.2 (d, J_{PP} = 8.4 Hz, 1P), −33.6 (s, 1P), −22.9 (dd, J_{PP} = 63.6, 8.4 Hz, 1P), −28.8 (d, J_{PP} = 63.6 Hz, 1P). Characterizing data for **7**: Anal. Calcd for $C_{46}H_{31}O_9Os_3P_3S_3$: C, 37.14; H, 2.10. Found: C, 37.39; H, 2.16. IR (CH_2Cl_2): ν_{CO} = 2064 w, 2000 s, 1980 vs, 1959 sh, 1936 m cm^{-1}. ^1H NMR ($CDCl_3$, 25 °C): δ = 7.55 (m, 3H), 7.46 (m, 3H), 7.33 (m, 20H), 7.16 (m, 3H), 4.96 (t, J = 10.6 Hz, 1H). $^{31}P\{^1H\}$ NMR ($CDCl_3$, 25 °C): δ = −24.6 (d, J_{PP} = 53.6 Hz, 1P), −27.6 (d, J_{PP} = 53.6 Hz, 1P), −43.4 (s, 1P). Characterizing data for **10**: Anal. Calcd for $C_{57}H_{40}O_8Os_3P_4S_6$: C, 39.35; H, 2.32. Found: C, 39.61; H, 2.39. IR (CH_2Cl_2): ν_{CO} = 2048 w, 1994 s, 1970 vs, 1931 m cm^{-1}. ^1H NMR ($CDCl_3$, 25 °C): aliphatic region: **10a**: δ = 4.68 (t, J = 10.4 Hz); **10b**: δ = 4.88 (t, J = 10.8 Hz), aromatic region: **10a**–**b**: δ = 7.49–6.88 (m). $^{31}P\{^1H\}$ NMR ($CDCl_3$, 25 °C): **10a**: δ = −20.7 (dd, J_{PP} = 50.2, 9.2 Hz), −27.3 (d, J_{PP} = 50.2 Hz), −39.3 (d, J_{PP} = 9.2 Hz), −51.8 (s); **10b**: δ = −29.1 (s), −40.8 (s).

4.3. Reaction of $[Os_3(CO)_8\{\mu_3\text{-}Ph_2PCH_2P(Ph)C_6H_4\}(\mu\text{-}H)]$ (**1**) with PFu_3

To a CH_2Cl_2 solution (20 mL) of **1** (50 mg, 0.042 mmol) was added PFu_3 (20 mg, 0.086 mmol) and the mixture was then stirred at 25 °C for 5 h. The solvent was removed under reduced pressure and the residue chromatographed by TLC on silica gel. Elution with hexane/CH_2Cl_2 (3:2, v/v) gave four bands which afforded the following compounds in order of elution: $[Os_3(CO)_{10}(\mu\text{-dppm})]$ (**2**) (3 mg, 6%) as yellow crystals, $[Os_3(CO)_8(PFu_3)\{\mu_3\text{-}Ph_2PCH_2P(Ph)C_6H_4\}(\mu\text{-}H)]$ (**5**) (7 mg, 12%) as yellow crystals, $[Os_3(CO)_9(PFu_3)(\mu\text{-dppm})]$ (**8**) (5 mg, 8%) as yellow crystals from hexane/CH_2Cl_2 at 4 °C and $[Os_3(CO)_8(PFu_3)_2(\mu\text{-dppm})]$ (**12**) (46 mg, 66%) as orange crystals from hexane/$C_2H_4Cl_2$ at 4 °C. Characterizing data for **5**: Anal. Calcd for $C_{45}H_{31}O_{11}Os_3P_3$: C, 38.29; H, 2.22. Found: C, 38.52; H, 2.26. IR (CH_2Cl_2): ν_{CO} = 2027 m, 2003 vs, 1991 s, 1956 m, 1935 m,br cm^{-1}. ^1H NMR ($CDCl_3$, 25 °C): δ = 8.14 (m, 1H), 7.19 (m, 18H), 6.89 (m, 1H), 6.69 (m, 2H), 6.65 (m, 2H), 6.40 (m, 1H), 6.35 (m, 1H), 6.06 (m, 1H), 5.90 (m, 1H), 5.33 (m, 1H), 3.61 (m, 1H), −18.36 (m, 1H). $^{31}P\{^1H\}$ NMR ($CDCl_3$, 25 °C): δ = −53.3 (s, 1P), −22.7 (d, J_{PP} = 67.2 Hz, 1P), −14.0 (d, J_{PP} = 67.2 Hz, 1P). Characterizing data for **8**: Anal. Calcd for $C_{46}H_{31}O_{12}Os_3P_3$: C, 38.38; H, 2.17. Found: C, 38.63; H, 2.23. IR (CH_2Cl_2): ν_{CO} = 2065 w, 2029 w, 2001 s, 1983 vs, 1967 sh, 1937

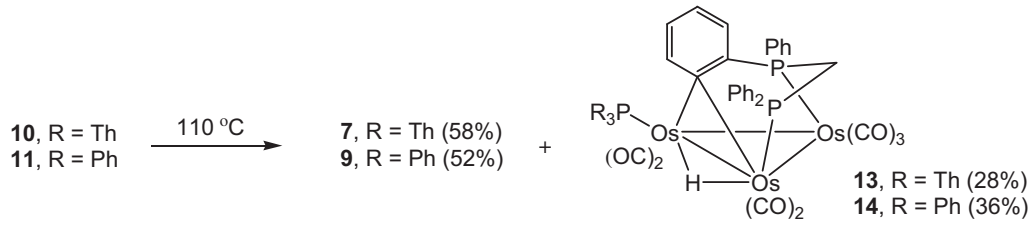

Scheme 4.

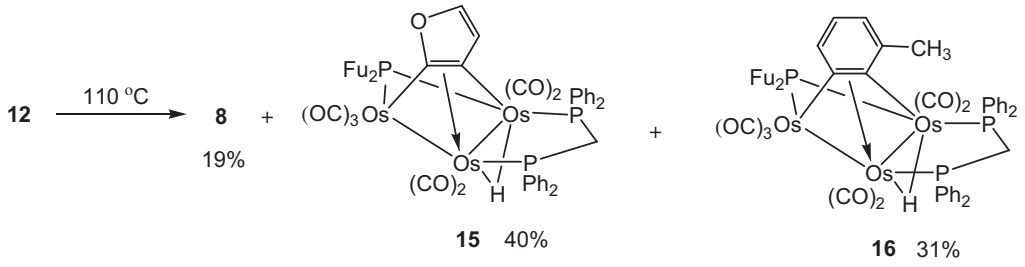

Scheme 5.

m cm^{-1}. ^1H NMR ($CDCl_3$, 25 °C): $\delta = 7.97$ (m, 2H), 7.69 (m, 2H), 7.65 (m, 2H), 7.51 (m, 2H), 7.34 (m, 15H), 6.88 (m, 2H), 6.69 (m, 2H), 6.45 (m, 2H), 4.33 (m, 1H), 4.20 (m, 1H). $^{31}P\{^1H\}$ NMR ($CDCl_3$, 25 °C): $\delta = -56.8$ (s, 1P), −27.4 (d, $J_{PP} = 53.4$ Hz, 1P), −24.8 (d, $J_{PP} = 53.4$ Hz, 1P). Characterizing data for **12**: Anal. Calcd for $C_{57}H_{40}O_{14}Os_3P_4$: C, 41.65; H, 2.46. Found: C, 41.86; H, 2.53. IR (CH_2Cl_2): ν_{CO} = 1993 s, 1967 vs, 1927 m cm^{-1}. ^1H NMR ($CDCl_3$, 25 °C): $\delta = 7.43$ (m, 6H), 7.31 (m, 20H), 6.47 (m, 6H), 6.28 (m, 6H), 4.87 (t, $J = 10.4$ Hz, 2H). $^{31}P\{^1H\}$ NMR ($CDCl_3$, 25 °C): $\delta = -28.3$ (s, 2P), −50.6 (s, 2P).

4.4. Reaction of $[Os_3(CO)_8\{\mu_3\text{-}Ph_2PCH_2P(Ph)C_6H_4\}(\mu\text{-}H)]$ (**1**) with PPh_3

PPh_3 (20 mg, 0.086 mmol) was added to a CH_2Cl_2 solution (20 mL) of **1** (50 mg, 0.042 mmol) and the mixture was then stirred at 25 °C for 7 h. The solvent was removed under reduced pressure and the residue subjected to TLC on silica gel for chromatographic separation. Elution with hexane/CH_2Cl_2 (7:3, v/v) gave four bands which afforded the following compounds in order of elution: $[Os_3(CO)_{10}(\mu\text{-dppm})]$ (**2**) (6 mg, 11%) as yellow crystals, $[Os_3(CO)_9(PPh_3)(\mu\text{-dppm})]$ (**9**) (12 mg, 19%) as yellow crystals, $[Os_3(CO)_8(PPh_3)_2(\mu\text{-dppm})]$ (**11**) (17 mg, 24%) as orange crystals and $[Os_3(CO)_8(PPh_3)\{\mu_3\text{-}Ph_2PCH_2P(Ph)C_6H_4\}(\mu\text{-}H)]$ (**6**) (18 mg, 29%) as yellow crystals after recrystallization from hexane/CH_2Cl_2 at 4 °C. Characterizing data for **9**: Anal. Calcd for $C_{52}H_{37}O_9Os_3P_3$: C, 42.50; H, 2.54. Found: C, 42.82; H, 2.61. IR (CH_2Cl_2): ν_{CO} = 2060 m, 2028 w, 1997 s, 1976 vs, 1964 sh, 1933 m cm^{-1}. ^1H NMR ($CDCl_3$, 25 °C): $\delta = 7.50$ (m, 6H), 7.35 (m, 29H), 4.93 (t, $J = 10.4$ Hz, 2H). $^{31}P\{^1H\}$ NMR ($CDCl_3$, 25 °C): $\delta = 0.8$ (s, 1P), −24.6 (d, $J_{PP} = 52.2$ Hz, 1P), −27.7 (d, $J_{PP} = 52.2$ Hz, 1P).

4.5. Thermolysis of $[Os_3(CO)_8(PTh_3)_2(\mu\text{-dppm})]$ (**10**)

A toluene solution (15 mL) of **10** (30 mg, 0.017 mmol) was heated to reflux for 3 h. The solvent was removed under reduced pressure and the residue separated by TLC on silica gel. Elution with hexane/CH_2Cl_2 (7:3, v/v) developed three bands. The first and second bands gave $[Os_3(CO)_9(PTh_3)(\mu\text{-dppm})]$ (**7**) (15 mg, 58%) as yellow crystals and $[Os_3(CO)_7(PTh_3)\{\mu_3\text{-}Ph_2PCH_2P(Ph)C_6H_4\}(\mu\text{-}H)]$ (**13**) (7 mg, 28%) as green crystals after recrystallization from hexane/CH_2Cl_2 at 4 °C. The third band gave a minor unidentified product. Characterizing data for **13**: Anal. Calcd for $C_{44}H_{31}O_7Os_3P_3S_3$: C, 36.91; H, 2.19. Found: C, 37.18; H, 2.24. IR (CH_2Cl_2): ν_{CO} = 2031 vs, 1990 vs, 1977 s, 1956 m, 1918 s cm^{-1}. ^1H NMR ($CDCl_3$, 25 °C): $\delta = 8.12$ (m, 1H), 7.89 (m, 2H), 7.60 (m, 15H), 7.11 (m, 3H), 6.98 (m, 3H), 6.56 (m, 1H), 6.23 (m, 2H), 6.15 (m, 1H), 4.78 (m, 1H), 3.77 (m, 1H), −12.16 (ddd, $J = 10.4$, 9.2, 1.8 Hz, 1H). $^{31}P\{^1H\}$ NMR ($CDCl_3$, 25 °C): $\delta = -15.1$ (d, $J_{PP} = 71.8$ Hz, 1P), −19.8 (d, $J_{PP} = 71.8$ Hz, 1P), −25.7 (s, 1P).

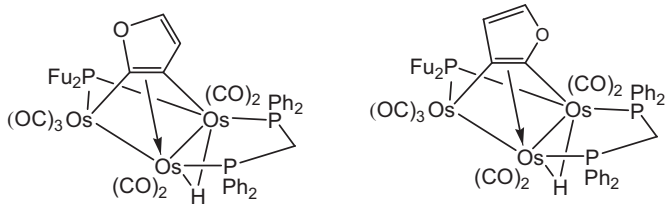

Chart 2.

4.6. Thermolysis of $[Os_3(CO)_8(PPh_3)_2(\mu\text{-dppm})]$ (**11**)

A toluene solution (15 mL) of **11** (40 mg, 0.023 mmol) was heated to reflux for 30 min. The solvent was removed by rotary evaporation and the residue chromatographed by TLC on silica gel. Elution with hexane/CH_2Cl_2 (7:3, v/v) developed three bands. The first and second bands gave $[Os_3(CO)_9(PPh_3)(\mu\text{-dppm})]$ (**9**) (18 mg, 52%) as yellow crystals and $[Os_3(CO)_7(PPh_3)\{\mu_3\text{-}Ph_2PCH_2P(Ph)C_6H_4\}(\mu\text{-}H)]$ (**14**) (12 mg, 36%) as green crystals after recrystallization from hexane/CH_2Cl_2 at 4 °C. The third band gave a minor unidentified product. Characterizing data for **14**: Anal. Calcd for $C_{50}H_{37}O_7Os_3P_3$: C, 42.48; H, 2.64. Found: C, 42.83; H, 2.72. IR (CH_2Cl_2): ν_{CO} = 2103 m, 2061 m, 2044 vs, 2012 s, 1964 w, 1940 w cm^{-1}. ^1H NMR ($CDCl_3$, 25 °C): $\delta = 7.95$ (m, 2H), 7.81 (m, 2H), 7.62 (m, 6H), 7.43 (m, 3H), 7.35 (m, 10H), 7.13 (m, 7H), 6.98 (m, 1H), 6.90 (m, 2H), 6.64 (m, 1H), 4.75 (m, 1H), 3.68 (m, 1H), −12.15 (ddd, $J = 18.4$, 10.8, 7.6 Hz, 1H). $^{31}P\{^1H\}$ NMR ($CDCl_3$, 25 °C): $\delta = 14.2$ (s, 1P), −14.7 (d, $J_{PP} = 74.5$ Hz, 1P), −20.5 (d, $J_{PP} = 74.5$ Hz, 1P).

4.7. Thermolysis of $[Os_3(CO)_8(PFu_3)_2(\mu\text{-dppm})]$ (**12**)

A toluene solution (15 mL) of **12** (30 mg, 0.018 mmol) was heated at 110 °C for 2 h. The solvent was removed by rotary evaporation and the residue separated by TLC on silica gel. Elution with hexane/CH_2Cl_2 (1:1, v/v) developed six bands. The second, third and fifth bands gave $[Os_3(CO)_7(\mu\text{-}PFu_2)(\mu_3\text{-}\eta^2\text{-}C_4H_2O)(\mu\text{-}H)(\mu\text{-dppm})]$ (**15**) (10 mg, 40%) as colorless crystals, $[Os_3(CO)_9(PFu_3)(\mu\text{-dppm})]$ (**8**) (5 mg, 19%) as yellow crystals and $[Os_3(CO)_7(\mu\text{-}PFu_2)(\mu_3\text{-}\eta^2\text{-}C_6H_3CH_3)(\mu\text{-}H)(\mu\text{-dppm})]$ (**16**) (8 mg, 31%) as colorless crystals after recrystallization from hexane/CH_2Cl_2 at 4 °C. The other three bands gave minor unidentified products. Characterizing data for **15**: Anal. Calcd for $C_{44}H_{31}O_{10}Os_3P_3$: C, 38.20; H, 2.26. Found: C, 38.43; H, 2.33. IR (CH_2Cl_2): ν_{CO} = 2055 s, 2031 s, 1998 s, 1980 s, 1957 sh cm^{-1}. ^1H NMR ($CDCl_3$, 25 °C): aliphatic region: **15a**: $\delta = 3.34$ (q, $J = 24.6$, 12.4 Hz), 2.53 (q, $J = 24.6$, 12.4 Hz); **15b**: $\delta = 3.10$ (q, $J = 24.0$, 11.8 Hz), 2.73 (q, $J = 24.0$, 11.8 Hz), aromatic region: **15a**–**b**: $\delta = 7.83$–6.36 (m), hydride region: **15a**: −17.31 (m); **15b**: −17.27 (m). $^{31}P\{^1H\}$ NMR ($CDCl_3$, 25 °C): **15a**: $\delta = 13.6$ (dd, $J_{PP} = 105.2$, 203.2 Hz), 8.0 (d, $J_{PP} = 105.2$ Hz), −92.6 (d, $J_{PP} = 203.2$ Hz); **15b**: $\delta = 10.2$ (dd, $J = 213.2$, 98.8 Hz), 4.4 (d, $J = 98.8$ Hz), −91.4 (d, $J_{PP} = 213.2$ Hz). ESI-MS: m/z = 1383 $[M^+-H]$. Characterizing data for **16**: Anal. Calcd for $C_{47}H_{35}O_9Os_3P_3$: C, 40.11; H, 2.51. Found: C,

Table 1
Crystal data and structure refinement for the complexes $[Os_3(CO)_8(PFu_3)\{\mu_3\text{-}Ph_2PCH_2P(Ph)C_6H_4\}(\mu\text{-}H)]$ (**5**), $[Os_3(CO)_9(PTh_3)(\mu\text{-dppm})]$ (**7**) and $[Os_3(CO)_9(PPh_3)(\mu\text{-dppm})]$ (**9**). $[Os_3(CO)_8(PTh_3)_2(\mu\text{-dppm})]$ (**10**), $[Os_3(CO)_8(PFu_3)_2(\mu\text{-dppm})]$ (**12**) and $[Os_3(CO)_7(PTh_3)\{\mu_3\text{-}Ph_2PCH_2P(Ph)C_6H_4\}(\mu\text{-}H)]$ (**13**). $[Os_3(CO)_7(PPh_3)\{\mu_3\text{-}Ph_2PCH_2P(Ph)C_6H_4\}(\mu\text{-}H)]$ (**14**), $[Os_3(CO)_7(\mu\text{-}PFu_2)(\mu^3\text{-}\eta^2\text{-}C_4H_2O)(\mu\text{-}H)(\mu\text{-dppm})]$ (**15**) and $[Os_3(CO)_7(\mu\text{-}PFu_2)(\mu_3\text{-}\eta^2\text{-}C_6H_3CH_3)(\mu\text{-}H)(\mu\text{-dppm})]$ (**16**).

	5.CH_2Cl_2	**7**	**9**.0.5 CH_2Cl_2
Chemical formula	$C_{46}H_{33}Cl_2O_{11}Os_3P_3$	$C_{46}H_{31}O_9Os_3P_3S_3$	$C_{52.50}H_{37.50}ClO_9Os_3P_3$
Formula mass	1496.13	1487.40	1511.28
Crystal system	Monoclinic	Monoclinic	Monoclinic
Space group	$P2_1/n$	C_2/c	C_2/c
a [Å]	15.616(4)	40.680(5)	41.535(6)
b [Å]	20.069(5)	11.386(1)	11.645(2)
c [Å]	15.846(4)	19.890(2)	20.206(3)
α°	90	90	90
β°	102.479(4)	92.453(2)	92.990(2)
γ°	90	90	90
Cell volume [Å^3]	4848(2)	9205(2)	9760(2)
Z	4	8	8
Calcd. density [g cm^{-3}]	2.050	2.147	2.057
Abs. coeff. μ [mm^{-1}]	8.109	8.558	8.002
F(000)	2816	5600	5716
Crystal color	Yellow	Orange	Orange
Crystal size [mm]	0.30 × 0.30 × 0.06	0.24 × 0.24 × 0.04	0.18 × 0.17 × 0.05
θ range for data collection [°]	2.62 to 28.29	2.75 to 28.30	2.29 to 28.31
Index ranges	$-19 \le h \ge 20$, $-25 \le h \ge 25$, $-20 \le h \ge 20$	$-54 \le h \ge 53$, $-15 \le h \ge 15$, $-26 \le h \ge 26$	$-55 \le h \ge 53$, $-15 \le h \ge 15$, $-26 \le h \ge 26$
Completeness to θ	99.6% to 26.00°	99.7% to 26.00°	99.5% to 26.00°
Reflections collected	40,924	39,109	40,686
Independent reflections	11,430 (R_{int} = 0.0892)	10,997 (R_{int} = 0.0521)	11,702 (R_{int} = 0.0461)
Min. and max. transmission	0.1947 and 0.6418	0.2332 and 0.7259	0.3268 and 0.6904
Data/restraints/parameters	11,430/0/596	10,997/0/575	11,702/0/621
Final R indices [$F^2 > 2\sigma$]	R_1 = 0.0484, wR_2 = 0.1246	R_1 = 0.0297, wR_2 = 0.0658	R_1 = 0.0308, wR_2 = 0.0731
R indices (all data)	R_1 = 0.0621, wR_2 = 0.1320	R_1 = 0.0367, wR_2 = 0.0683	R_1 = 0.0378, wR_2 = 0.0757
Goodness-of-fit on F^2	1.045	1.029	1.033
Largest diff. peak and hole [e.Å^{-3}]	4.254 and−2.117	1.404 and−1.431	1.803 and−1.942
	10.1.5 CH_2Cl_2	**12**.CH_2Cl_2.4H_2O	**13**.$CHCl_3$
Chemical formula	$C_{58.5}H_{43}Cl_3O_8Os_3P_4S_6$	$C_{59}H_{52}Cl_2O_{18}Os_3P_4$	$C_{45}H_{32}Cl_3O_7Os_3P_3S_3$
Formula mass	1867.12	1814.39	1550.75
Crystal system	Monoclinic	Triclinic	Monoclinic
Space group	$P2_1/n$	P 1 bar	$P2_1$/c
a [Å]	23.143(4)	12.099(2)	13.424(4)
b [Å]	21.980(3)	15.578(2)	19.906(5)
c [Å]	24.468(4)	19.092(3)	18.093(5)
α°	90	76.243(2)	90
β°	98.651(2)	72.173(2)	90.885(4)
γ°	90	86.758(2)	90
Cell volume [Å^3]	12,305(3)	3327.0(8)	4834(2)
Z	8	2	4
Calcd. density [g cm^{-3}]	2.016	1.811	2.131
Abs. coeff. μ [mm^{-1}]	6.672	5.957	8.309
F(000)	7144	1744	2920
Crystal color	Orange	Orange	Red
Crystal size [mm]	0.46 × 0.16 × 0.13	0.42 × 0.12 × 0.04	0.46 × 0.42 × 0.12
θ range for data collection [°]	1.13 to 28.31	2.38 to 28.26	2.47 to 28.33
Index ranges	$-30 \le h \ge 30$, $-29 \le h \ge 29$, $-32 \le h \ge 31$	$-16 \le h \ge 16$, $-20 \le h \ge 20$, $-24 \le h \ge 24$	$-17 \le h \ge 17$, $-26 \le h \ge 26$, $-23 \le h \ge 24$
Completeness to θ	99.8% to 26.00°	97.6% to 26.00°	99.8% to 26.00°
Reflections collected	1,04,259	28,233	39,578
Independent reflections	29,564 (R_{int} = 0.0498)	15,110 (R_{int} = 0.0458)	11,407 (R_{int} = 0.0740)
Min. and max. transmission	0.1493 and 0.4775	0.1887 and 0.7966	0.1146 and 0.4355
Data/restraints/parameters	29,564/0/1466	15,110/2/775	11,407/0/568
Final R indices [$F^2 > 2\sigma$]	R_1 = 0.0439, wR_2 = 0.1082	R_1 = 0.0635, wR_2 = 0.1971	R_1 = 0.0508, wR_2 = 0.1271
R indices (all data)	R_1 = 0.0541, wR_2 = 0.1141	R_1 = 0.0731, wR_2 = 0.2172	R_1 = 0.0613, wR_2 = 0.1333
Goodness-of-fit on F^2	1.037	0.977	1.041
Largest diff. peak and hole [e.Å^{-3}]	3.094 and−1.768	4.738 and−3.600	4.184 and−1.884
	14.1.5CH_2Cl_2	**15**	**16**.2CH_2Cl_2
Chemical formula	$C_{52}H_{41}Cl_3O_7Os_3P_3$	$C_{46}H_{31}O_9Os_3P_3$	$C_{98}H_{78}Cl_8O_{16}Os_6P_6$
Formula mass	1547.71	1391.22	3154.23
Crystal system	Triclinic	Triclinic	Triclinic
Space group	P 1 bar	P 1 bar	P 1 bar

Table 1 (*continued*)

	14.1.5CH_2Cl_2	**15**	**16**.2CH_2Cl_2
a [Å]	10.487(2)	10.0797(6)	12.085(2)
b [Å]	15.456(3)	11.7563(7)	12.219(2)
c [Å]	16.719(3)	19.667(1)	38.384(6)
α°	90.899(3)	79.920(1)	94.299(3)
β°	99.824(3)	76.121(1)	92.388(3)
γ°	107.982(3)	67.817(1)	119.605(2)
Cell volume [$Å^3$]	2533.0(8)	2085.8(2)	4894(1)
Z	2	2	2
Calcd. density [g cm^{-3}]	2.029	2.215	2.140
Abs. coeff. μ [mm^{-1}]	7.810	9.289	8.143
F(000)	1466	1304	2984
Crystal color	Green	Yellow	Yellow
Crystal size [mm]	0.12 × 0.12 × 0.03	0.16 × 0.08 × 0.06	0.24 × 0.17 × 0.08
θ range for data collection [°]	2.58 to 28.32	2.07 to 28.28	1.07 to 28.28
Index ranges	$-13 \le h \ge 13$, $-20 \le h \ge 19$, $-22 \le h \ge 22$	$-13 \le h \ge 12$, $-15 \le h \ge 15$, $-24 \le h \ge 25$	$-16 \le h \ge 15$, $-16 \le h \ge 16$, $-50 \le h \ge 50$
Completeness to θ	97.3% to 26.00°	97.2% to 26.00°	97.2% to 26.00°
Reflections collected	21,849	17,296	41,880
Independent reflections	11,542 (R_{int} = 0.0453)	9207 (R_{int} = 0.0362)	22,249 (R_{int} = 0.0344)
Min. and max. transmission	0.4542 and 0.7995	0.3180 and 0.6057	0.2454 and 0.5620
Data/restraints/parameters	11,542/0/603	9207/0/541	22,249/0/1204
Final *R* indices [$F^2 > 2\sigma$]	R_1 = 0.0460, wR_2 = 0.1011	R_1 = 0.0362, wR_2 = 0.0718	R_1 = 0.0466, wR_2 = 0.1378
R indices (all data)	R_1 = 0.0740, wR_2 = 0.1233	R_1 = 0.0527, wR_2 = 0.0780	R_1 = 0.0585, wR_2 = 0.1545
Goodness-of-fit on F^2	1.032	0.986	1.037
Largest diff. peak and hole [e.$Å^{-3}$]	2.035 and−1.689	2.667 and−2.297	2.405 and−2.246

40.33; H, 2.56. IR (CH_2Cl_2): ν_{CO} = 2061 s, 2032 s, 2008 s, 1987 s, 1971 s cm^{-1}. ^{1}H NMR ($CDCl_3$, 25 °C): δ = 7.62 (m, 3H), 7.51 (m, 1H), 7.45 (m, 3H), 7.23–7.03 (m, 13H), 6.97 (m, 2H), 6.83 (m, 2H), 6.74 (m, 1H), 6.59 (m, 1H), 6.41 (m, 1H), 6.39 (m, 1H), 6.32 (m, 1H), 3.26 (dd, *J* = 24.6, 12.4 Hz, 1H), 2.50 (dd, *J* = 24.6, 12.4 Hz, 1H), 1.57 (s, 3H, Me), −17.22 (dt, *J* = 10.8, 7.6 Hz, 1H). ^{31}P{^{1}H} NMR ($CDCl_3$, 25 °C): δ = 19.2 (dd, J_{PP} = 111.6, 210.9 Hz, 1P), 5.8 (d, J_{PP} = 111.6 Hz, 1P), −98.0 (d, J_{PP} = 210.9 Hz, 1P). ESI-MS: *m*/*z* = 1411 [M^+−H].

4.8. X-ray crystallography

Single crystals of **5**, **7**, **9**, **10**, **13**, **14**, **15** and **16** suitable for X-ray structure analysis were grown by slow diffusion of hexane into dichloromethane solution at 4 °C and that of **12** by slow diffusion of hexane into dichloroethane solution at 4 °C. Diffraction intensities were collected at 150(2) K with a Bruker SMART APEX2 CCD diffractometer using Mo-Kα radiation (λ = 0.71073 Å). Indexing and initial cell refinements as well as the data collection were all done using APEX2 [22] software. Data integration was accomplished with SAINT [23] software and numerical absorption correction (based on the real shape of the crystals) followed by scaling procedure with SADABS program [24] were used to account for systematic effects. The structures were solved by direct methods [25] and refined by full-matrix least squares [26]. In most of the structures all non-hydrogen atoms were refined anisotropically and hydrogen atoms were included using a riding model. The structure of **5** contains a dichloromethane molecule in which one of the chlorine atoms is disordered [Cl(2A)/Cl(2B)] and protons were not generated for this. In **7**, the sulfur-carbon atoms on one of the thienyl groups are disordered over two sites. Cluster **9** co-crystallized with half a molecule of dichloromethane, the chlorine atom of which makes a close contact (3.226 Å) with one of the carbonyl oxygen atoms, O(3). For this complex, all hydrogen atoms were located from difference maps and refined isotropically. The asymmetric unit of **10** contains two triosmium clusters and three molecules of dichloromethane. There are short contacts of 2.87–3.05 Å between oxygen atoms of the carbonyl ligands while one oxygen atom has a short contact with a sulfur atom on a neighboring molecule [O(2)-S(10) 3.204 Å]. Four carbon atoms in thienyl rings, namely C(27), C(47), C(59) and C(63), were refined only isotropically. The asymmetric unit of **12** contains a disordered molecule of dichloromethane and four extra unconnected peaks in the difference map which have been modeled as oxygen atoms (presumably from water). Hydrogen atoms were not placed on any of these solvent molecules. The asymmetric unit of **13** contains a disordered molecule of chloroform. Cluster **14** co-crystallized with one and a half molecules of dichloromethane, the half molecule being disordered over two sites. Both were refined only isotropically and protons were not included for the disordered molecule. For **16** there were two clusters and four molecules of dichloromethane in the asymmetric unit. In one of the solvent molecules a chlorine atom was equally disordered over two sites [Cl(8) and Cl(9)]. These atoms were refined only isotropically and protons were not generated. Scattering factors were taken from International Tables for X-ray Crystallography [27]. Crystallographic data are given in Table 1.

4.9. Computational methodology

DFT calculations were performed with the Gassian09 package of programs [28]. The calculations were carried out with the B3LYP functional, which utilizes the Becke three-parameter exchange functional (B3) [29] combined with the correlation functional of Lee, Yang, and Parr (LYP) [30]. The osmium atoms were described by Stuttgart–Dresden effective core potentials (ecp) and an SDD basis set, while the 6–31G(d′) basis set was employed for the remaining atoms. The geometry-optimized structures were drawn with the *JIMP*2 molecular visualization and manipulation program [31].

Acknowledgments

This research has been partly sponsored by The Ministry of Education, Government of the Peoples Republic of Bangladesh. SG

thanks the Commonwealth Scholarship Commission for the award of a Commonwealth Scholarship. GH thanks The Royal Society of Chemistry for an International Authors Award which allowed him to complete this manuscript while visiting the University of North Texas. MGR acknowledges financial support from the Robert A. Welch Foundation (Grant B-1093) and the NSF (CHE-0741936). Prof. Michael B. Hall (TAMU) is thanked for providing us a copy of his *JIMP2* program, which was used to prepare the geometry-optimized structures reported here. We also thank Ms. Anna Gould who was supported by a Nuffield Foundation Undergraduate Research Bursary for the VT NMR study of $[Os_3(CO)_8(PTh_3)_2(\mu\text{-dppm})]$.

Appendix A. Supplementary material

CCDC 941629, 941630, 941631, 941632, 941634, 941633, 941635, 941636 and 941637 contain the supplementary crystallographic data for this paper. These data can be obtained free of charge from The Cambridge Crystallographic Data Centre via www.ccdc.cam.ac.uk/data_request/cif.

References

[1] G. Hogarth, S.E. Kabir, E. Nordlander, Dalton Trans. 39 (2010) 6153–6174.
[2] (a) A. Okrut, O. Gazit, N. De Silva, R. Nichiporuk, A. Solovyov, A. Katz, Dalton Trans. 41 (2012) 2091–2099;
(b) R.D. Adams, S. Wang, Organometallics 5 (1986) 1274–1276;
(c) R.R. Burch, A.J. Shusterman, E.L. Muetterties, R.G. Teller, J.M. Williams, J. Am. Chem. Soc. 105 (1983) 3546–3556;
(d) M.D. Fryzuk, Organometallics 1 (1982) 408–409;
(e) F.W. Heinemann, H.-C. Böttcher, J. Organomet. Chem. 526 (1996) 145–147.
[3] (a) S.A. MacLaughlin, N.J. Taylor, A.J. Carty, Organometallics 3 (1984) 392–399;
(b) F. Van Gastel, S.A. MacLaughlin, M. Lynch, A.J. Carty, E. Sappa, A. Tiripicchio, M. Tiripicchio Camellini, J. Organomet. Chem. 326 (1987) C65–C70;
(c) S.G. Bott, H. Shen, M.G. Richmond, J. Organomet. Chem. 690 (2005) 3838–3845;
(d) D. Blazina, S.B. Duckett, P.J. Dyson, J.A.B. Lohman, J. Chem. Soc. Dalton Trans. (2004) 2108–2114;
(e) M. Lanfranchi, A. Tiripicchio, E. Sappa, A.J. Carty, J. Chem. Soc. Dalton Trans. (1986) 2737–2740.
[4] (a) A. Bertolucci, M. Freni, P. Romiti, G. Ciani, A. Sironi, V.G. Albano, J. Organomet. Chem. 113 (1976) C61–C64;
(b) T. Beringhelli, G. Ciani, G. D'Alfonso, H. Molinari, A. Sironi, Inorg. Chem. 24 (1985) 2666–2671;
(c) T. Beringhelli, C. Ciani, G. D'Alfonso, M. Freni, J. Organomet. Chem. 311 (1986) C51–C54;
(d) T. Beringhelli, G. D'Alfonso, M. Freni, G. Ciani, M. Moret, A. Sironi, J. Organomet. Chem. 339 (1988) 323–332;
(e) T. Beringhelli, G. D'Alfonso, M. Freni, G. Ciani, M. Moret, A. Sironi, J. Organomet. Chem. 399 (1990) 291–299;
(f) T. Beringhelli, G. D'Alfonso, A.P. Minoja, G. Ciani, M. Moret, A. Sironi, Organometallics 10 (1991) 3131–3138.
[5] (a) T. Beringhelli, G. D'Alfonso, A. Minoja, G. Ciani, D.M. Proserpio, Inorg. Chem. 32 (1993) 803–810;
(b) T. Beringhelli, G. Ciani, G. D'Alfonso, H. Molinari, J. Chem. Soc. Chem. Commun. (1987) 486–488;
(c) R. Saillant, G. Barcelo, H.D. Kaesz, J. Am. Chem. Soc. 92 (1970) 5739–5741;
(d) R.D. Wilson, R. Bau, J. Am. Chem. Soc. 98 (1976) 4687–4689.
[6] (a) T. Jaeger, S. Aime, H. Vahrenkamp, Organometallics 5 (1986) 245–252;
(b) T. Jaeger, H. Vahrenkamp, Organometallics 7 (1988) 1746–1752;
(c) W. Wang, J.F. Corrigan, G.D. Enright, N.J. Taylor, A.J. Carty, Organometallics 17 (1998) 427–432;
(d) J.T. Jaeger, A.K. Powell, H. Vahrenkamp, New J. Chem. 12 (1988) 405–408;
(e) J.T. Jaeger, A.K. Powell, H. Vahrenkamp, Chem. Ber. 121 (1988) 1729–1738.
[7] (a) R.J. Puddephatt, Lj. Manojlovic-Muir, K.W. Muir, Polyhedron 9 (1990) 2767–2802;
(b) P.D. Harvey, K. Hierso, P. Braunstein, X. Morise, Inorg. Chim. Acta 250 (1996) 337–343;
(c) M.C. Jennings, N.C. Payne, R.J. Puddephatt, Inorg. Chem. 26 (1987) 3776–3781;
(d) B.R. Lloyd, A. Bradford, R.J. Puddephatt, Organometallics 6 (1987) 424–427;
(e) J. Xiao, E. Kristof, J.J. Vittal, R.J. Puddephatt, J. Organomet. Chem. 490 (1995) 1–6;
(f) F. Cimadevilla, M.E. Garcia, D. Garcia-Vivo, M.A. Ruiz, C. Graiff, A. Tiripicchio, Inorg. Chem. 51 (2012) 10427–10436.
[8] (a) S.E. Kabir, D.S. Kolwaite, E. Rosenberg, K. Hardcastle, W. Cresswell, J. Grindstaff, Organometallics 14 (1995) 3611–3613;
(b) A.M. Joynal, B. Bergman, R. Holmquist, R. Smith, E. Rosenberg, J. Ciurash, K. Hardcastle, J. Roe, V. Vazquez, C. Roe, S. Kabir, B. Roy, S. Alam, K.A. Azam, Coord. Chem. Rev. 190-192 (1999) 975–1002;
(c) Md.I. Hossain, S. Ghosh, G. Hogarth, G.M.G. Hossain, S.E. Kabir, J. Organomet. Chem. 696 (2011) 3036–3039;
(d) A.K. Raha, Md.R. Hassan, S.E. Kabir, Md.M. Karim, B.K. Nicholson, A. Sharmin, L. Salassa, E. Rosenberg, J. Clust. Sci. 19 (2008) 47–62;
(e) N. Begum, D.W. Bennett, G.M.G. Hossain, S.E. Kabir, A. Sharmin, D.T. Haworth, T.A. Siddiquee, E. Rosenberg, J. Clust. Sci. 16 (2005) 413–428;
(f) Md.A. Mottalib, N. Begum, S.M.T. Abedin, T. Akter, S.E. Kabir, Md.A. Miah, D. Rokhsana, E. Rosenberg, G.M.G. Hossain, K.I. Hardcastle, Organometallics 24 (2005) 4747–4759;
(g) S. Ghosh, Md.R. Al-Mamun, G.M.G. Hossain, S.E. Kabir, Inorg. Chim. Acta 378 (2011) 307–310;
(h) B. Bergman, R. Holmquist, R. Smith, E. Rosenberg, J. Ciurash, K. Hardcastle, M. Visi, J. Am. Chem. Soc. 120 (1998) 12818–12828;
(i) E. Arcia, D.S. Kolwaite, E. Rosenberg, K. Hardcastle, J. Ciurash, R. Duque, R. Gobetto, L. Milone, D. Osella, M. Botta, W. Dastru, A. Viale, I. Fiedler, Organometallics 17 (1998) 415–426;
(j) S.E. Kabir, H. Vahrenkamp, M.B. Hursthouse, K.M.A. Malik, J. Organomet. Chem. 536–537 (1997) 509–517;
(k) S. Ghosh, Md.N. Uddin, N. Begum, G.M.G. Hossain, K.A. Azam, S.E. Kabir, J. Chem. Crystallogr. 40 (2010) 572–578;
(l) Kh.M. Uddin, S. Ghosh, A.K. Raha, G. Hogarth, E. Rosenberg, A. Sharmin, K.I. Hardcastle, S.E. Kabir, J. Organomet. Chem. 695 (2010) 1435–1440.
[9] (a) R.D. Adams, B. Captain, Angew. Chem. Int. Ed. Engl. 44 (2005) 2531–2533;
(b) R.D. Adams, B. Captain, C. Beddie, M.B. Hall, J. Am. Chem. Soc. 129 (2007) 986–1000;
(c) R.D. Adams, B. Captain, L. Zhu, J. Organomet. Chem. 693 (2008) 819–833;
(d) R.D. Adams, B. Captain, P.J. Pellechia, Organometallics 26 (2007) 6564–6575;
(e) R.D. Adams, B. Captain, Angew. Chem. Int. Ed. Engl. 46 (2007) 5714–5716;
(f) R.D. Adams, E.M. Boswell, M.B. Hall, X. Yang, Organometallics 27 (2008) 4938–4947.
[10] (a) A.J. Deeming, Adv. Organomet. Chem. 26 (1986) 1–96;
(b) A.J. Deeming, S. Hasso, M. Underhill, J. Chem. Soc. Dalton Trans. (1975) 1614–1620;
(c) W.G. Jackson, B.F.G. Johnson, J.W. Kelland, J. Lewis, K.T. Schorpp, J. Organomet. Chem. 87 (1975) C27–C30;
(d) J.B. Keister, J.R. Shapley, J. Organomet. Chem. 85 (1975) C29–C31;
(e) H.D. Kaesz, S.A.R. Knox, J.W. Koepke, R.B. Saillant, J. Chem. Soc. Chem. Commun. (1971) 477;
(f) M.R. Churchill, F.J. Hollander, J.P. Hutchinson, Inorg. Chem. 16 (1977) 2697–2700;
(g) R.B. Calvert, J.R. Shapley, J. Am. Chem. Soc. 99 (1977) 5225–5226;
(h) A. Gonzalez-Hernandez, S. Hernandez-Ortega, E. Gomez, J.M. Fernandez-G, J. Organomet. Chem. 696 (2011) 3436–3439;
(i) S.K. Brayshaw, L.P. Clarke, P. Homanen, O.F. Koentjoro, J.E. Warren, P.R. Raithby, Organometallics 30 (2011) 3955–3965;
(j) J.A. Cabeza, I. del Rio, J.M. Fernandez-Colinas, E. Perez-Carreno, M.G. Sanchez-Vega, D. Vazquez-Garcia, Organometallics 29 (2010) 3828–3836;
(k) O.A. Kizas, S.Y. Erdyakov, D.Y. Antonov, I.A. Godovikov, E.V. Vorontsov, F.M. Dolgushin, M.G. Ezernitskaya, I.G. Barakovskaya, New J. Chem. 33 (2009) 1760–1770;
(l) C.E. Cooke, M.C. Jennings, M.J. Katz, R.K. Pomeroy, J.A.C. Clyburne, Organometallics 27 (2008) 5777–5799;
(m) N. Begum, U.K. Das, M. Hassan, G. Hogarth, S.E. Kabir, E. Nordlander, M.A. Rahman, D.A. Tocher, Organometallics 26 (2007) 6462–6472;
(n) M.J. Stchedroff, V. Moberg, E. Rodriguez, A.E. Aliev, J. Boettcher, J.W. Steed, E. Nordlander, M. Monari, A.J. Deeming, Inorg. Chim. Acta 359 (2006) 926–937.
[11] (a) J.A. Clucas, D.F. Foster, M.M. Harding, A.K. Smith, J. Chem. Soc. Chem. Commun. (1984) 949–950;
(b) J.A. Clucas, M.M. Harding, A.K. Smith, J. Chem. Soc. Chem. Commun. (1985) 1280–1281.
[12] S.E. Kabir, G. Hogarth, Coord. Chem. Rev. 253 (2009) 1285–1315.
[13] (a) J.A. Clucas, P.A. Dolby, M.M. Harding, A.K. Smith, J. Chem. Soc. Chem. Commun. (1987) 1829–1831;
(b) R.A. Bartlett, C.J. Cardin, D.J. Cardin, G.A. Lawless, J.M. Power, P.P. Power, J. Chem. Soc. Chem. Commun. (1988) 312–313;
(c) M.P. Brown, P.A. Dolby, M.M. Harding, M.A. Mathews, A.K. Smith, D. Osella, M. Arbrun, R. Gobetto, P.R. Raithby, P. Zanello, J. Chem. Soc. Dalton Trans. (1993) 827–834;
(d) M.P. Brown, P.A. Dolby, M.M. Harding, A.J. Mathews, A.K. Smith, J. Chem. Soc. Dalton Trans. (1993) 1671–1679;
(e) M.M. Harding, B. Kariuki, A.J. Mathews, A.K. Smith, P. Braunstein, J. Chem. Soc. Dalton Trans. (1994) 33–36;
(f) K.A. Azam, M.B. Hursthouse, M.R. Islam, S.E. Kabir, K.M.A. Malik, R. Miah, C. Sudbrake, H. Vahrenkamp, J. Chem. Soc. Dalton Trans. (1998) 1097–1105;
(g) S.M.T. Abedin, K.I. Hardcastle, S.E. Kabir, K.M.A. Malik, M.A. Mottalib, E. Rosenberg, M.J. Abedin, Organometallics 19 (2000) 5623–5627;
(h) S.E. Kabir, K.M.A. Malik, E. Molla, M.A. Mottalib, J. Organomet. Chem. 616 (2000) 157–164;
(i) S.E. Kabir, C.A. Johns, K.M.A. Malik, M.A. Mottalib, E. Rosenberg, J. Organomet. Chem. 625 (2001) 112–120;

(j) S.E. Kabir, N. Begum, H.Md. Manjur, H.Md. Hyder, H. Nur, D.W. Bennett, T.A. Siddiquee, D.T. Haworth, E. Rosenberg, J. Organomet. Chem. 689 (2004) 1569–1579;
(k) A.J. Deeming, M.M. Hassan, S.E. Kabir, E. Nordlander, D.A. Tocher, J. Chem. Soc. Dalton Trans. (2004) 3709–3714;
(l) S.E. Kabir, Md.A. Miah, N.C. Sarker, G.M.G. Hossain, K.I. Hardcastle, D. Rokhsana, E. Rosenberg, J. Organomet. Chem. 690 (2005) 3044–3053;
(m) S.M. Azad, K.A. Azam, S.E. Kabir, M.S. Saha, G.M.G. Hossain, J. Organomet. Chem. 690 (2005) 4206–4211;
(n) M.R. Hassan, G. Hogarth, G.M.G. Hossain, S.E. Kabir, A.K. Raha, M.S. Saha, D.A. Tocher, Organometallics 26 (2007) 6473–6480;
(o) A.K. Raha, S. Ghosh, Md.M. Karim, D.A. Tocher, N. Begum, A. Sharmin, E. Rosenberg, S.E. Kabir, J. Organomet. Chem. 693 (2008) 3613–3621;
(p) A.K. Raha, S. Ghosh, S.E. Kabir, B.K. Nicholson, D.A. Tocher, J. Organomet. Chem. 694 (2009) 752–756;
(q) A.K. Raha, S. Ghosh, I. Hossain, S.E. Kabir, B.K. Nicholson, G. Hogarth, L. Salassa, J. Organomet. Chem. 696 (2011) 2153–2160.
[14] S.-H. Huang, J.M. Keith, M.B. Hall, M.G. Richmond, Organometallics 29 (2010) 4041–4057.
[15] (a) W.-Y. Wong, F.-L. Ting, W.-L. Lam, Eur. J. Inorg. Chem. (2002) 2103–2111;
(b) W.-Y. Wong, F.-L. Ting, Z. Lin, Organometallics 22 (2003) 5100–5108;
(c) S. Ghosh, M. Khatun, D.T. Haworth, S.V. Lindeman, T.A. Siddiquee, D.W. Bennett, G. Hogarth, E. Nordlander, S.E. Kabir, J. Organomet. Chem. 694 (2009) 2941–2948;
(d) S. Karmaker, S. Ghosh, S.E. Kabir, D.T. Haworth, S.V. Lindeman, Inorg. Chim. Acta 382 (2012) 199–202;
(e) Md. A. Rahman, N. Begum, S. Ghosh, Md. K. Hossain, G. Hogarth, D.A. Tocher, E. Nordlander, S.E. Kabir, J. Organomet. Chem. 696 (2011) 607–612;
(f) N. Begum, M.A. Rahman, M.R. Hassan, S.E. Kabir, E. Nordlander, G. Hogarth, D.A. Tocher, J. Organomet. Chem. 693 (2008) 1645–1655;
(g) W.-Y. Wong, F.-L. Ting, W.-L. Lam, J. Chem. Soc. Dalton Trans. (2001) 2981–2988;
(h) C. Santelli-Rouvier, C. Coin, L. Toupet, M. Santelli, J. Organomet. Chem. 495 (1995) 91–96;
(i) S. Ghosh, G. Hogarth, S.E. Kabir, E. Nordlander, L. Salassa, D.A. Tocher, J. Organomet. Chem. 696 (2011) 1982–1989;
(j) M.I. Hossain, M.D.H. Sikder, S. Ghosh, S.E. Kabir, G. Hogarth, L. Salassa, Organometallics 31 (2012) 2546–2558.
[16] (a) N.G. Anderson, B.A. Keay, Chem. Rev. 101 (2001) 997–1030;
(b) M. Sakai, H. Hayashi, N. Miyaura, Organometallics 16 (1997) 4229–4231;
(c) E. Shirakawa, K. Yamasaki, T. Hiyama, Synthesis (1998) 1544–1549;
(d) B.M. Trost, Y.H. Rhee, J. Am. Chem. Soc. 121 (1999) 11680–11683;
(e) J.C. Anderson, H. Namli, C.A. Roberts, Tetrahedron 53 (1997) 15123–15134;
(f) W.A. Herrmann, S. Brossmer, K. Öfele, M. Beller, H. Fischer, J. Mol. Catal. A Chem. 103 (1995) 133–146;
(g) V. Farina, S.R. Baker, D.A. Benigni, C. Sapino, Tetrahedron Lett. 29 (1988) 5739–5742;
(h) I. Klement, M. Rottländer, C.E. Tucker, T.N. Majid, P. Knochel, P. Venegas, G. Cahiez, Tetrahedron 52 (1996) 7201–7220.
[17] (a) S. Ghosh, S. Rana, D.A. Tocher, G. Hogarth, E. Nordlander, S.E. Kabir, J. Organomet. Chem. 694 (2009) 3312–3319;
(b) M.N. Uddin, N. Begum, M.R. Hassan, G. Hogarth, S.E. Kabir, M.A. Miah, E. Nordlander, D.A. Tocher, J. Chem. Soc. Dalton Trans. (2008) 6219–6230;
(c) U. Bodensieck, H. Varenkamp, G. Rheinwald, H. Stoeckli-Evans, J. Organomet. Chem. 488 (1995) 85–90;
(d) N.K. Kiriakidou Kazemifar, M.J. Stchedroff, M.A. Mottalib, S. Selva, M. Monari, E. Nordlander, Eur. J. Inorg. Chem. (2006) 2058–2068;
(e) A.J. Deeming, M.K. Shinhmar, A.J. Arce, Y.De. Sanctis, J. Chem. Soc. Dalton Trans. (1999) 1153–1160;
(f) A.J. Deeming, S.N. Jaysuriya, A.J. Arce, Y.De. Sanctis, Organometallics 15 (1996) 786–793;
(g) M.A. Mottalib, S.E. Kabir, D.A. Tocher, A.J. Deeming, E. Nordlander, J. Organomet. Chem. 692 (2007) 5007–5016;
(h) M.N. Uddin, M.A. Mottalib, N. Begum, S. Ghosh, A.K. Raha, D.T. Haworth, S.V. Lindeman, T.A. Siddiquee, D.W. Bennett, G. Hogarth, E. Nordlander, S.E. Kabir, Organometallics 28 (2009) 1514–1523;
(i) J.D. King, M. Monari, E. Nordlander, J. Organomet. Chem. 573 (1999) 272–278;
(j) S. Ghosh, G. Hogarth, D.A. Tocher, E. Nordlander, S.E. Kabir, Inorg. Chim. Acta 363 (2010) 1611–1614;
(k) S. Ghosh, A.K. Das, N. Begum, D.T. Haworth, S.V. Lindeman, J.F. Gardinier, T.A. Siddiquee, D.W. Bennett, E. Nordlander, G. Hogarth, S.E. Kabir, Inorg. Chim. Acta 362 (2009) 5175–5182;
(l) A. Rahaman, F.R. Alam, S. Ghosh, M. Haukka, S.E. Kabir, E. Nordlander, G. Hogarth, J. Organomet. Chem. 730 (2013) 123–131;
(m) M. Ackermann, A. Pascariu, T. Höcher, H.-U. Siehl, S. Berger, J. Am. Chem. Soc. 128 (2006) 8434–8440.
[18] S.R. Hodge, B.F.G. Johnson, J. Lewis, P.R. Raithby, J. Chem. Soc. Dalton Trans. (1987) 931–937.
[19] K.A. Azam, M.B. Hursthouse, M.R. Islam, S.E. Kabir, K.M.A. Malik, R. Miah, C. Sudbrake, H. Vahrenkamp, J. Chem. Soc. Dalton Trans. (1998) 1097–1105.
[20] K.A. Azam, M.B. Hursthouse, S.E. Kabir, K.M.A. Malik, M.A. Mottalib, J. Chem. Crystallogr. 29 (1999) 813–818.
[21] X. Zhang, S. Kandala, L. Yang, W.H. Watson, X. Wang, D.A. Hrovat, W.T. Borden, M.G. Richmond, Organometallics 30 (2011) 1253–1268.
[22] *APEX2* Version 2.0-2, Bruker AXS, Inc., Madison, WI, 2005.
[23] *SAINT* Version 7.23A, Bruker AXS, Inc., Madison, WI, 2005.
[24] G. Sheldrick, *SADABS* Version 2004/1, University of Göttingen, 2004.
[25] Program XS from *SHELXTL* Package, V. 6.12, Bruker AXS, Inc., Madison, WI, 2001.
[26] Program XL from *SHELXTL* Package, V. 6.12, Bruker AXS, Inc., Madison, WI, 2001.
[27] A.J.C. Wilson (Ed.), International Tables for X-ray Crystallography, vol. C, Kynoch, Academic Publishers, Dordrecht, 1992, pp. 219–222. Tables 6.1.1.4 (pp. 500–502) and 4.2.6.8.
[28] M.J. Frisch, et al., Gaussian 09, Revision E.01, Gaussian, Inc., Wallingford, CT, USA, 2009.
[29] A.D. Becke, J. Chem. Phys. 98 (1993) 5648.
[30] C. Lee, W. Yang, R.G. Parr, Phys. Rev. B 37 (1993) 785.
[31] (a) M.B. Hall, R.F. Fenske, JIMP2, version 0.091, a free program for the visualization and manipulation of molecules, Inorg. Chem. 11 (1972) 768;
(b) J. Manson, C.E. Webster, M.B. Hall, Texas A&M University, College Station, TX, 2006. http://www.chem.tamu.edu/jimp2/index.html.